nuclear weapons journal

Issue 1 2006

- Dynamic Response of Plutonium
- Davis Gun Experiments
- Modeling Permeability Development
- Compressive Response of Kel-F 800
- HE Replacement

Contents

About the cover: In this plate dent test, a cylinder of explosive was fitted with a detonator, mounted vertically on a thick cold-rolled steel plate, and detonated from the top. The depth of the dent in the plate after detonation indicates the explosive's relative power. This type of test can be used to study properties of a variety of energetic materials.

We proudly dedicate this issue of the *Journal* to Robert W. Kuckuck the eighth and final director of Los Alamos National Laboratory under the management of the University of California. Dr. Kuckuck's tenure, while all too brief, will long be remembered for his steady leadership, compassion, sense of humor, and emphasis on scientific and engineering excellence. Oppenheimer would be pleased.

"A man is the sum of his actions, of what he has done, of what he can do, nothing else." Gandhi

Issue 1, 2006 LALP-06-084

Nuclear Weapons Journal highlights ongoing work in the nuclear weapons program at Los Alamos National Laboratory. *NWJ* is an unclassified, quarterly publication funded by the Nuclear Weapons Program Directorate.

Managing Editor-Science Writer
Margaret Burgess

Science Writer-Editors
Larry McFarland
Jan Torline

Designer-Illustrator
Randy Summers

Editorial Advisor
Jonathan Ventura

Technical Advisor
Sieg Shalles

Printing Coordinator
Lupe Archuleta

Send inquiries, comments, and address changes to *nwpub@lanl.gov* or to
The Nuclear Weapons Journal
Los Alamos National Laboratory
Mail Stop A121
Los Alamos, NM 87545

Point of View

Little Boy to RRW—the University of California and Los Alamos

Robert W. Kuckuck
Former Director
Los Alamos National Laboratory

On May 31, 2006, the University of California completed a 63-year period of serving the nation as the sole manager of Los Alamos National Laboratory. On June 1, UC began a new period of managing the Laboratory in a partnership with private-sector companies. It is interesting to reflect upon UC's contributions to the nation's nuclear weapons program during this era that began with Little Boy and is ending with the development of the Reliable Replacement Warhead (RRW).

There are remarkable parallels between Little Boy and current RRW concepts:

- the weapon will not be tested
- the design is extremely conservative
- its designers have high confidence in its performance
- the design emphasizes relative ease of fabrication
- its designers rely heavily on calculations and small-scale experiments rather than on testing
- the success of the design is highly dependent upon understanding of weapons science.

Neither of these projects could have been possible without the world-class science that UC has brought to bear at Los Alamos from the beginning. UC has endowed the Laboratory with immense scientific credibility and capability—entrée into the highest levels of the world's science community, access to the best of peer review, and collaborations at the forefront of science. The pragmatic result for the weapons program has been the ability to attract, motivate, and retain the best talent available. There is no doubt that the largest components underpinning the unparalleled success of the nation's nuclear force in World War II and the nuclear deterrent in the cold war and beyond are the depth, breadth, and quality of the science upon which our nuclear defense is based.

UC established a standard for public service that is unparalleled in the areas of national defense and weapons.

In addition to providing science and technology to address nuclear weapons programmatic objectives, UC has also established a model for the appropriate role of an academic institution that serves in the public interest. UC voluntarily provided the organizational framework and many key personnel to help the Manhattan Project achieve its technical objectives, without significant reward and with some sacrifice of its own critical resources. UC has continued to foster a sense of public service and intellectual independence that has provided the nation credible, outspoken, and objective scientific counsel of unquestioned integrity.

UC established a standard for public service that is unparalleled in the areas of national defense and weapons. There is little doubt that the current federal model for ensuring the safety and reliability of the nation's nuclear stockpile, an annual certification process that relies upon the directors of the weapons design laboratories to personally vouch for the viability of stockpiled nuclear weapon systems, is credible only because of the objectivity and independence of the research staff at the weapons

continued on page 28

New Suitable Replacement for the High-Temperature Explosive HNS-4

Explosives with high thermal stability have a wide variety of applications in military, space, and civilian uses. A frequent civilian application, for example, is the use of such explosives in shaped charges that explosively perforate downhole well pipe and penetrate surrounding rock to improve oil recovery. The explosive in these downhole penetrators should have a high detonation velocity (V_D, km/s) and detonation pressure (P_{CJ}, kbar) and must withstand high temperatures and still initiate and perform reliably. The same is true for military and space applications in which explosives are subjected to high temperatures. We have prepared and thoroughly tested a high-temperature, insensitive explosive (HTIX), 2,4,8,10-tetranitro-5H-pyrido[3',2':4,5][1,2,3]-triazolo[1,2-a]benzotriazol-6-ium inner salt or 2,4,8,10-tetranitro-benzopyrido-1,3a,6,6a-tetraaza-pentalene (BPTAP), that is an attractive replacement for HTIXs currently being used in applications that require high thermal stability.

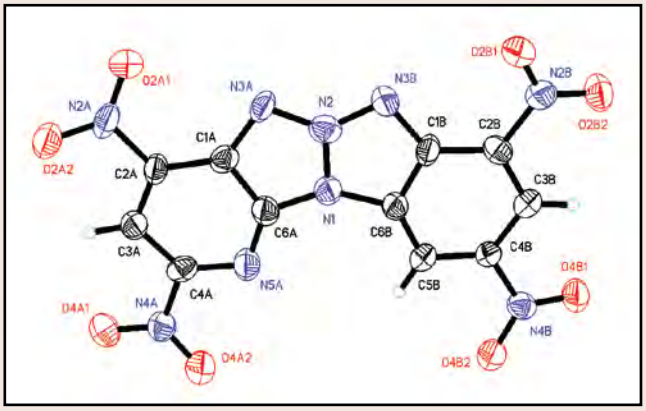

Oak Ridge Thermal Ellipsoid Plot (ORTEP) diagram (25% ellipsoids) for BPTAP. ORTEP is the computer program for drawing thermal crystal structure illustrations (motion probability ellipsoids). The individual element labels identify elements and enable discussion of the locations and lengths of specific bonds.

An HTIX called HNS (2,2',4,4',6,6'-hexanitrostilbene) is commonly used in such applications because it is stable and is readily prepared by the oxidative coupling of TNT by hypochlorite. And the most commonly used HNS compound is HNS-4, recrystallized four times using dimethylformamide (DMF) as the solvent.

But HNS-4 has a number of disadvantages that offset its relative ease of preparation. It requires a lengthy purification process involving recrystallization from DMF, a toxic solvent that poses expensive and time-consuming waste-disposal problems. In addition, HNS-4 displays relatively poor performance with its detonation velocity of 7.07 km/s and detonation pressure of only 199 kbar at a density of 1.685 g/cm^3 (96.8% of theoretical maximum density of 1.740). An explosive with higher detonation velocity and pressure would be desirable. Furthermore, the HNS-4 differential scanning calorimetry exotherm (DSC Exo) of 315°C is too low to be completely reliable for some high-temperature applications. The DSC Exo of a material is the temperature at which a reaction occurs to release heat: the higher the DSC Exo the better so that the explosive will be thermally stable at high temperatures.

Much attention in HTIX research has been focused on the preparation (precursors and methods) and properties of the class of explosives known as heterocyclic tetraazapentalenes (TAPs) and their derivatives because of their thermal stability, performance, and practicality of synthesis. Our interest in heterocyclic TAPs led us to investigate their explosive performance (V_D and P_{CJ}) to develop candidates with better performance than is offered by HTIXs currently in use. After investigating a variety of TAPs, we focused on and investigated the synthesis and explosive properties of BPTAP.

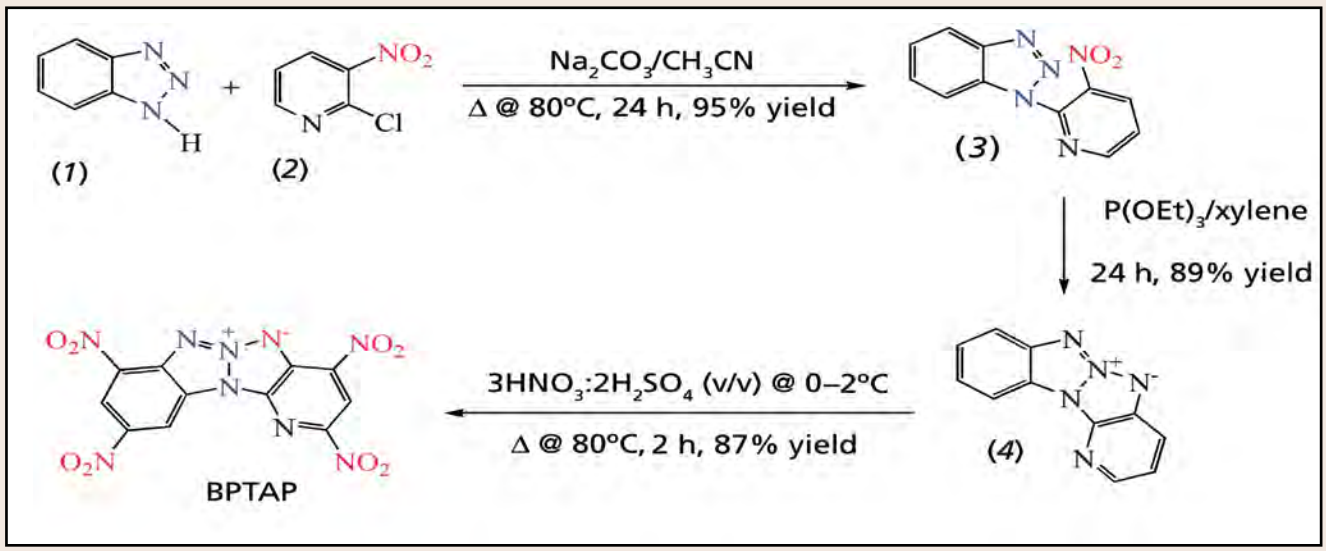

The preparation of BPTAP is straightforward. The condensation reaction between benzotriazole (*1*) and 2-chloro-3-nitroporidine (*2*) occurs in acetonitrile containing sodium carbonate (Na_2CO_3) to give a positional regioisomer (*3*), which undergoes a ring closure reaction to give the other possible regioisomer (*4*). After dissolution in 98% sulfuric acid (H_2SO_4) at 5°C, 90% nitric acid (HNO_3) is slowly added while the temperature is maintained below 2°C. With vigorous stirring, the reaction mixture is heated to 80°C for 2 h, cooled to room temperature, and poured onto crushed ice. Once filtered and washed with cold water, the yellow product is consecutively triturated with minimum amounts of acetone, acetonitrile, and methanol to wash off the remaining acids.

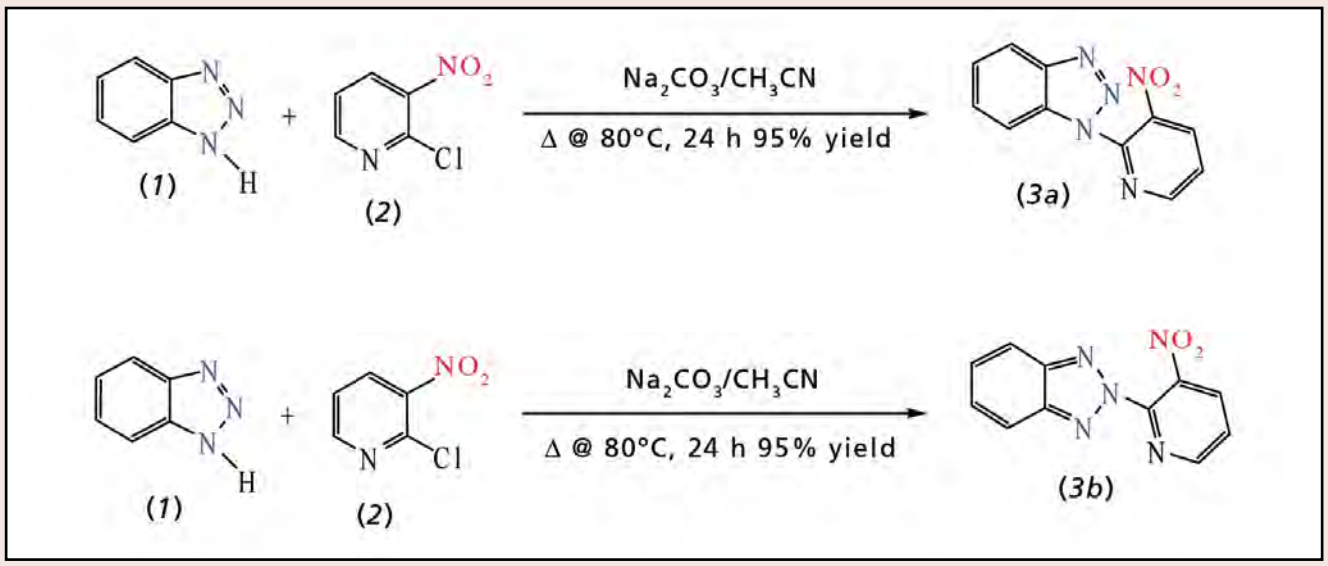

This graphic illustrates the role of regioisomers in the preparation of BPTAP. Isomers are chemical compounds that have the same number and type of each atom but different arrangements of those atoms, resulting in differing physical and/or chemical properties. A regioisomer is the isomer product that a chemical reaction favors over other possible isomer products. The condensation reaction between benzotriozole (*1*) and 2-chloro-3-nitropyridine (*2*) in the preparation of BPTAP could favor the production of the regioisomers (*3a*) or (*3b*), or a mixture of the two. In fact, this reaction gives only (*3a*) and not (*3b*) at all.

We characterized BPTAP by x-ray crystallography and by UV-visible, infrared, ^1H, and ^{13}C nuclear magnetic resonance spectroscopies. Its physical and chemical properties were determined by DSC Exo and heat of formation; its explosive performance was measured for V_D and P_{CJ} at 1.78 g/cm³ density; and its energetic sensitivities were evaluated by friction, spark, and drop height (impact). The density from x-ray crystal structure is 1.868 g/cm³, and the heat of formation, measured by combustion calorimetry,

This 1.75-mm-diameter dent in a steel plate was caused by a BPTAP explosive detonation. The plate dent test provides a relative measurement of detonation pressure. The test was developed at the Explosive Research Laboratory in Bruceton, Pennsylvania, and was then refined at Los Alamos. An explosive cylinder is fitted at the top with a detonator and mounted vertically on a cold-rolled steel plate thick enough so that it will not be distorted (a stack of several plates is often used). The depth of the dent (in this case 2.3 mm) indicates the explosive's relative power (detonation pressure).

is a very attractive +106 kcal/mol (+443.5 kJ/mol). The DSC Exo of fast decomposition at 375°C indicates that BPTAP is more thermally stable than HNS-4 (and more stable than explosives such as TACOT and PYX, discussed later). BPTAP is insensitive to initiation by friction and spark. Its impact sensitivity was determined in drop hammer tests to be 59 cm (type 12); for comparison, the drop height sensitivity for HNS-4 is 54 cm.

The BPTAP V_D of 7.43 km/s and P_{CJ} of 294 kbar were determined by a rate stick-plate dent test using a stack of five 0.5-in. pellets at density 1.78 g/cm³ (95.3% of the theoretical maximum density from the x-ray crystal density measurement of 1.868 g/cm³). In addition, a poly-rho test was performed to determine detonation velocity as a function of density; test results show that there is very little degradation in velocity at an explosive diameter of 6.35 mm in the rate stick. The poly-rho test is an explosive rate stick composed of explosive pellets of increasing density, detonated at the low-density end of the rate stick to measure the detonation velocity of the explosive at different densities.

In the combined rate stick-plate dent experiment, we used a stack of five cylindrical 0.5-in.-diameter by 0.5-in.-long pellets of BPTAP. We fitted the stack with a detonator, mounted it vertically on a 2-in.-thick mild steel plate, and fired the detonator. Five electrical wires spaced along the stack shorted out when the detonation wave front arrived at each one, providing a measure of the detonation rate. The depth of the dent in the steel plate created by the detonation provided a measure of the detonation pressure. And explosive failure diameters can be determined by fabricating rate sticks of decreasing diameters until the smallest stick fails to sustain a detonation.

BPTAP offers significant advantages over HNS-4 as an HTIX. It is insensitive to initiation by spark and friction and has a drop height of 59 cm; when it is formulated with 5 wt% of the copolymer Kel-F 800 as a binder, the drop height increases to 155 cm. BPTAP is easier and cheaper to prepare in a three-step process without any purification and recrystallization, has a higher thermal stability (its DSC Exo of fast decomposition is 375°C versus 315°C for HNS-4), and has a faster V_D (7.43 km/s versus 7.07 km/s) and a higher P_{CJ} (294 kbar versus 199 kbar). Its failure diameter is at least as low as 3 mm, as determined by rate stick-plate dent tests. The failure diameter is the minimum cylindrical diameter of explosive needed to propagate a detonation wave, so a very small failure diameter is desirable in an explosive. As a consequence of its characteristics, BPTAP is a perfect candidate for HNS-4 replacement.

Why BPTAP in particular? We considered a variety of other thermally stable, insensitive explosives in the course of our investigations. A compound called PYX [2,6-bis(picrylamino)-3,5-dinitropyridine], a LANL-developed HTIX, has excellent thermal stability (DSC Exo at 350°C), but the synthesis requires the use of an expensive picryl halide.

Comparison between HNS-4 and BPTAP

Characteristics	HNS-4	BPTAP	Compare BPTAP with HNS-4
Maximum density	1.740 g/cm^3	1.868 g/cm^3	Higher
Heat of formation	+78.2 kJ/mol or +18.7 kcal/mol	+443.5 kJ/mol or +106 kcal/mol	~5.7 times better
Thermal stability	315°C DSC Exo	375°C DSC Exo	Higher
Detonation velocity	7.07 km/s at 1.69 g/cm^3 density	7.43 km/s at 1.78 g/cm^3 density	Better performance
Detonation pressure	199 kbar at 1.69 g/cm^3 density	294 kbar at 1.78 g/cm^3 density	Better performance
Friction initiation	>36 kg (insensitive)	>36 kg (insensitive)	Comparable
Spark initiation	>0.36 kg (insensitive)	>0.36 kg (insensitive)	Comparable
Impact sensitivity	54 cm	59 cm	Less sensitive
Failure diameter	<1 mm	<3 mm[a]	Comparable

[a] We do not have the required die to press the explosive pellets for rate stick-plate dent tests to measure failure diameter to less than 3 mm. In any case, the failure diameter of BPTAP is desirably very small.

We considered explosives called PPTAPs and BBTAPs, but did not study them because of material supply, preparation, and waste disposal issues.

We studied explosives called TACOTs. *Z*-TACOT (1,3,7,9-tetranitro-6*H*-benzotriazolo[2,1-a]benzotriazol-5-ium inner salt) and *T*- or *T*-TACOT (2,4,8,10-tetranitro-5H-benzotriazolo[1,2-a]benzotriazol-6-ium inner salt), DSC Exo at 354°C, were the first members we studied of a family of thermally stable explosives based on the TAP ring structure. Although these TACOTs are highly stable TAPs, their chromatographical separations and lengthy purifications have made their production expensive. Researchers have prepared derivatives of TACOTs in an effort to increase performance by improving the oxygen balance, density, and heat of formation. This increase was accomplished by substituting nitrogen for carbon in the benzene rings. Unfortunately, these derivative compounds are expensive to manufacture because the starting 1,2,3-triazolo-pyridines are not readily available. However, an interesting hybrid structure containing both a benzene and pyridine ring was reported by Belgian workers. They reported that this new material, BPTAP, had a melting point >300°C, but reported no explosive properties data. Because this compound is easy to prepare and offers promising thermal stability, it was our choice.

Our BPTAP reaction sequence gives 73.6% yield, which is two and one-half times more than the yield previously reported by the Belgian researchers. In addition, our nitration process is much shorter (2 h versus 48 h), and both solvents (acetonitrile from the BPTAP condensation reaction and xylenes from the ring closure step) are distilled to recover them for reuse. Compared with the most commonly used HTIXs, BPTAP is in the upper range of thermal stability, and it has the highest experimentally measured detonation velocity and pressure. The combination of better reaction yield, cheaper production cost, and higher performance makes BPTAP attractive for realistic and yet practical HTIX applications. NWJ

Points of contact:
My Hang V. Huynh, 667-9668, huynh@lanl.gov
Michael A. Hiskey, 667-4592, hiskey@lanl.gov

Also contributing to this research by determining sensitivity and performance properties of BPTAP were Ernest Hartline, Herbert Harry, Dennis Montoya, and Jose Archuleta of the Materials Dynamics Group, and M. S. Campbell, retired.

Davis Gun Experimental Simulation of Severe Mechanical Environments

Impact deceleration events are challenging to measure and quantify. However, the Davis gun project team can simulate deceleration events by tailoring acceleration events in which experimental variables can be controlled. This research is timely because an experimental method that successfully simulates decelerations for test articles weighing up to 2,000 lb would have significant application in a wide range of severe impact and vibration environments for weapon development and certification.

The 2-in. Davis gun suspended on a ballistic pendulum. The reaction mass protrudes from the gun barrel on the right. Accelerometer wires attached to the noses of the projectile and reaction mass led to oscilloscopes, and the two wires near the middle of the gun were for pressure transducer measurements. The ignition wires are not shown. The 4-in. grid behind the gun shows any movement of the gun during a shot and provides a reference background for real-time video.

Several experimental methods for weapon testing can simulate large deceleration environments for short duration (2–3 ms). However, few experimental methods are available to simulate large deceleration environments for long duration (intervals of at least 10 ms).

In large-caliber guns, the launch accelerations of the projectiles are repeatable to within a few percent from shot to shot, making them a very useful experimental tool for studying severe mechanical environments. We define a severe mechanical environment as a deceleration of full-scale components or subsystems of up to 2,000 times the force of gravity (2,000 *g's*) for 10 ms. The Davis gun is commonly used for earth-penetrating weapon (EPW) development.

A Davis gun is recoilless because it fires two masses simultaneously out of each end of an open gun tube: a projectile is fired out of one end of the gun, and a reaction mass is fired out of the other end.

The technical goal of our research is to determine if a Davis gun launch environment can be tailored to simulate the severe mechanical environment of an EPW impact event. In principle, if acceleration rise time could be shortened and a superposition of pressure pulses could produce a constant acceleration for 5–10 ms, the Davis gun could generate a nearly square-wave acceleration pulse, which would be an excellent simulation of an EPW impact

The Davis gun four-tube charge bank assembly. Each tube, loaded with black powder, could be fired independently. The charge bank was 12 in. long and fit inside the 2-in.-i.d. Davis gun.

The reaction mass (*top*) and projectile (*bottom*) fired from the Davis gun, with accelerometer wires attached to their nose cones. The reaction mass weighed 12.3 lb and the projectile weighed 3.9 lb. Each had three lengthwise grooves for phenolic resin runners that provided support in the gun barrel and reduced friction. Plastic disks (not shown) at the base ends of the reaction mass and projectile acted as pressure seals.

deceleration event. That is, on impact an EPW experiences a sudden deceleration that, when graphed, rises quickly to an amplitude that persists for 5–10 ms and then abruptly falls to zero.

Historically, Sandia National Laboratories (SNL) maintained and operated the Davis guns used in Nuclear Weapons Complex programs. The SNL Davis guns are now maintained and operated by the Energetic Materials Research and Testing Center (EMRTC) of the New Mexico Institute of Mining and Technology (NM Tech) in Socorro, New Mexico. SNL has 8-, 12-, and 16-in.-bore guns. EMRTC has its own 2-, 6-, and 15-in. Davis guns. Applied Research Associates Inc. also participates in the Davis gun tests at NM Tech. The SNL/EMRTC Davis gun capability is unique in the US.

For our feasibility study, we performed a five-shot subscale Davis gun test series at EMRTC with an approximately 60-in.-long EMRTC gun that had a 2-in. bore. The gun was hung on a ballistic pendulum to provide a qualitative check that the momentums of the projectile and reaction mass were balanced.

To generate a superposed pressure pulse to tailor the projectile and reaction mass launch accelerations, the team designed and built a 12-in.-long, four-tube charge bank to fit inside the 2-in. Davis gun tube. The charge bank was similar to a multiple rocket motor assembly with four parallel propellant tubes, one or more of them loaded with black powder. Each tube in the charge bank could be loaded and fired independently of the other three tubes. For each shot, we loaded a charge bank and inserted it into the gun tube between the projectile and the reaction mass. The charge bank attached to the gun tube with two bolts screwed into the barrel from the outside surface of the gun. A hole drilled through one of the attachment bolts provided wiring access into each propellant tube. Very light end caps closed the ends of the charge bank tubes. We ignited the multiple tubes of the charge bank in sequence using an individual fire set for each tube, timed with a Stanford signal generator.

Each shot in the test series fired a projectile and reaction mass. We used a machined projectile shape as reaction mass because we wanted to take pressure, acceleration, video (against a lattice background), and other measurements from it as well as from the projectile. We designed both the projectile and reaction mass as cone-nosed soil penetrators and fabricated them from 304 stainless steel. The projectile weighed 3.9 lb and the reaction mass weighed 12.3 lb. We instrumented both the projectile and reaction mass with accelerometers to measure axial launch accelerations.

In each shot, we fired the projectile and the reaction mass into two plywood boxes that were 4 ft in each dimension. The boxes were open at the top and were filled with sand. In each shot, we recorded both high-speed video and real-time video. Additional test instrumentation measured the ignition times and timing delays and the approximate times that the projectile exited the gun barrel and impacted the outer surface of the target box. All tests used FFF black powder. The F designations for black powder indicate the screen sizes—and resultant grain sizes—used in manufacturing the black powder, with FFF being smaller and faster-burning than F and FF. The five-shot test series included shots that fired one, two, and three tubes of the charge bank with ignition delays of up to 5.0 ms:

- Test 1: single charge
- Test 2: two charges, no ignition delay, pulse superposition

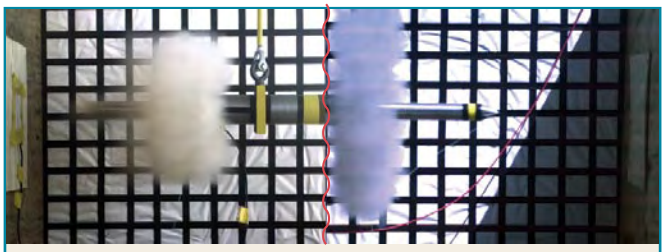

A typical composite high-speed video photograph showing the projectile (*left*) and reaction mass (*right*) just after they exited the Davis gun tube. The black powder gases appear to be of different colors because of differences in the available lighting. The real-time video showed that the Davis gun exhibited little to no pendulum motion during the five test shots, indicating that the momentums of the projectile and reaction mass were balanced.

Video photograph showing the projectile as it exited the Davis gun tube. The shroud of hot propellant gases enveloping the projectile made video measurements difficult; in fact, the reaction mass provided better measurements because its nose cone already protruded from the gun barrel before firing and so traversed clear air ahead of propellant gases.

- Test 3: two charges, one at a 3.5-ms ignition delay, pulse superposition
- Test 4: two charges, one at a 5.0-ms ignition delay, pulse superposition
- Test 5: three charges, two at 5.0-ms ignition delays, pulse superposition.

When the reaction mass was loaded into the Davis gun, its nose protruded from the end of the gun tube and was visible from time zero forward. Therefore, we obtained good displacement (position-time) measurements for the reaction mass from the high-speed video on all five tests. No direct position-time data were obtained for the projectile from the high-speed video. This was expected because the projectile was inside the barrel for almost the entire time interval of interest, and when the projectile did emerge, it was shrouded in propellant gases.

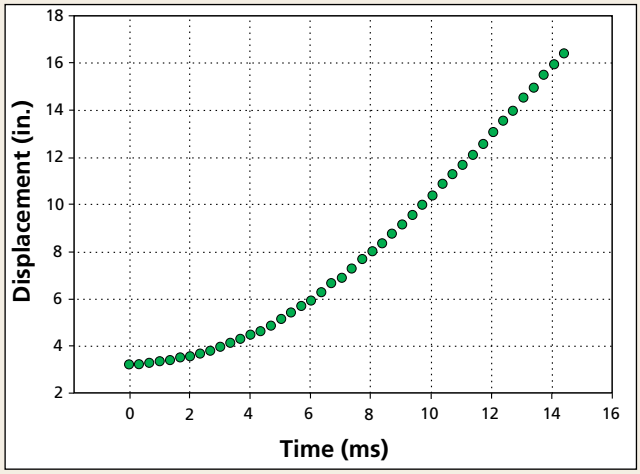

Measured reaction mass displacement in inches from the Davis gun barrel as a function of ignition time in milliseconds. For this shot, two tubes of the charge bank were fired with a 5.0-ms delay. Displacement data are useful because reaction mass velocity can be computed from such data.

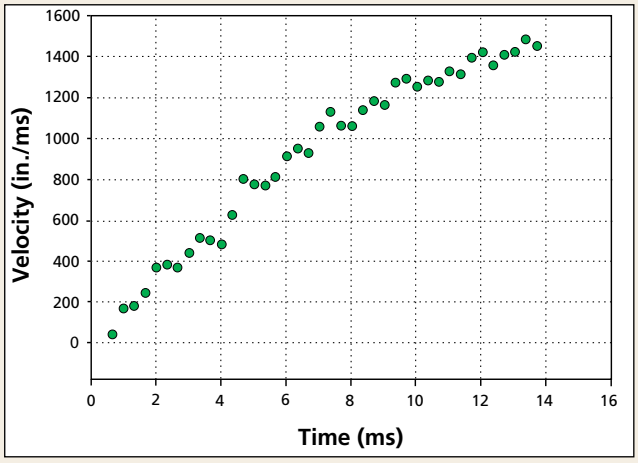

Reaction mass velocity computed from displacement data for a shot in which two tubes of the charge bank were fired with a 5.0-ms delay. Scatter in the velocity approximation is attributable to jitter in the video position-time data.

Because the subscale Davis gun shots exhibited little recoil on the real-time video, the motion of the projectile can be closely estimated from the motion of the reaction mass by assuming that the momentums of projectile and reaction mass are equal. We used a symmetrical, four-point, finite-difference formula to compute the velocity of the reaction mass. The scatter in the velocity approximation is due to jitter in the visual position-time data. Applying the velocity estimate to the projectile, assuming that

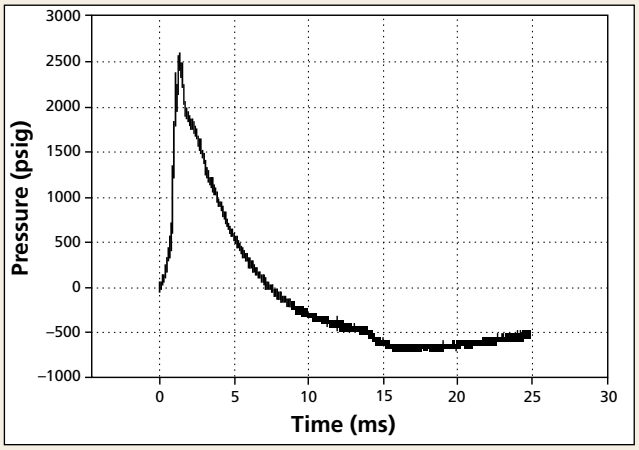

Measured Davis gun chamber pressure for a shot in which one tube of the charge bank was fired to provide a baseline for multiple-tube shots. Of particular interest here is the pressure rise time because it is one of the variables we want to tailor to simulate an acceleration square wave.

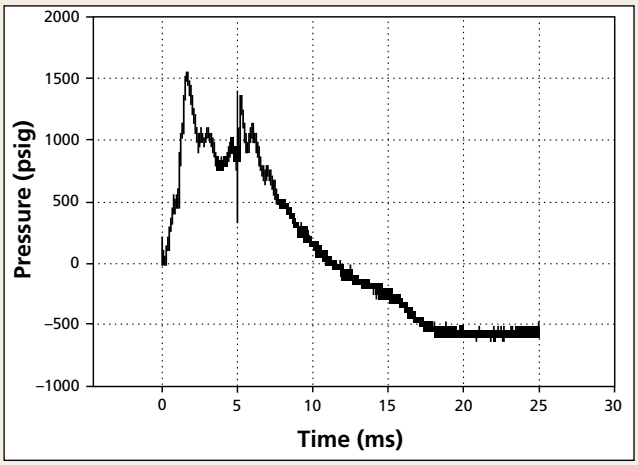

Measured Davis gun chamber pressure for a shot in which two tubes of the charge bank were fired with a 5.0-ms delay. Fast-burning black powder is fired in two or more tubes to achieve both a rapid rise time and pressures that remain high for up to 10 ms. The goal of tailoring the pressure pulse is to produce an acceleration pulse that approximates a square wave such as occurs during projectile earth-penetration deceleration.

the momentums of the projectile and reaction mass are equal, indicates that the projectile experienced an average acceleration of around 1,100 *g's* over the first 3 ms of the shot in test 4.

In addition to the position-time data, we measured time-dependent gun chamber pressures for each shot in the test series. We used two pressure transducers in the Davis gun chamber, one located near the initial position of the projectile base and one located near the initial position of the reaction mass base. The pressure data show that the initial rise time of the pressure pulse can be shortened as a function of the propellant amount and burn rate. The pressure data also show that the charge bank design allows individual propellant tubes to be ignited with timing delays to produce superposed pressure pulses. The decrease of the pressure rise time and the use of ignition timing delays and pressure pulse superposition indicate that a 2-in. Davis gun tube acceleration pulse may indeed be modified to have some of the features of an idealized square-wave acceleration pulse.

The next step in this research will be to tailor a specified pressure pulse by using timing delays and pressure superposition. This approach will provide insight into how to generate a gun tube acceleration pulse that approximates a square wave. In concert with the pressure pulse tailoring, research will begin to extend the charge bank concept and design to a 6-in. Davis gun.

The severe mechanical environment of interest will be simulated by the launch acceleration in the gun tubes using a reverse ballistics technique. The test articles will be oriented backwards along the centerline inside the projectiles fired from the Davis guns. The test projectile will be shot into a soft target, inducing a well-defined deceleration on the projectile and test article of a substantially lower magnitude than the gun tube launch acceleration. To test EPW components, a reliable soft catch target can be constructed from layered plywood and sand. A 6-in. Davis gun will allow projectiles large enough in diameter to carry self-contained data recorders and test small components and materials samples in severe mechanical environments. NWJ

Point of contact:
Roy S. Baty, 667-9319, rbaty@lanl.gov

Also contributing to this research were Ron Lundgren of Applied Research Associates Inc.; Garth Reader of the Applied Electromagnetics Group; and Lawrence Brooks and Peter Sandoval of the Weapons Systems Engineering Group.

Project Management Implementation for LANL Nuclear Weapons Programs

Can you name the world's largest project? If you guessed the Great Pyramid of Cheops or the Great Wall of China, you would be mistaken—it was the Manhattan Project, which consumed about 1% of the entire globe's resources in the years 1944–1945. That being so, you may believe that the management of projects stemming from the creation of the first nuclear weapons would be rather advanced.

Interestingly, however, project management and nuclear weapons technology were born at about the same time. Within a few years of Marie Curie's realizing that pitchblende was more radioactive than could be explained by its uranium content alone, Henry Gantt was studying management processes associated with the construction of naval vessels.

Traditional management techniques focused on maximizing shareholder wealth, but these techniques were almost useless when the goal was to complete a project within customer constraints of time and cost. Gantt realized that large projects could—and should—be broken down into smaller components. He also realized that those components were linked; i.e., some activities had to be completed before others could begin. Today these components and links are known as activities and schedule logic, and they are traditionally reported in a Gantt chart. When this scheduling technique was combined with the cost performance method known as earned value (EV)—the methodology used to assess cost and schedule performance—modern project management was born.

However, a common sticking point for research and development projects involved the difficulty of capturing an entire set of project outputs and outcomes, known as "scope," because the outcome of experiments and research can determine scope. Using project management to estimate the cost and schedule of research work was perceived as analogous to asking Columbus to describe the New World before he sailed.

In spite of this obstacle, as the nation's nuclear laboratories systematically outpaced the rest of the world in technology, their need for project management information systems increased dramatically. The Soviet Union was spending from 12% to 14% of its gross national product on defense during the late 1960s and 1970s—two to three times the amount the United States was spending. In short, to maintain its technological edge, the United States needed a management edge.

> Project management correlates cost, schedule, and performance data.

Implementing an earned-value management system (EVMS) across any nuclear weapons program includes

- changing the way mangers approach allocating and estimating needed financial, equipment, and personnel resources for their projects and
- resolving the enormous difficulties of capturing vague, indistinct scope into specific, trackable baselines.

These challenges make project management implementation particularly difficult in a large research organization such as Los Alamos. It became the perfect anti-EVMS storm for the Laboratory, yet one that the Program Controls Office of the Principal Associate Directorate for Nuclear Weapons Programs (PADNWP) had to overcome. Beginning in July 2004, Project Management Division and PADNWP personnel captured and decomposed LANL's Nuclear Weapons Program scope in a master work breakdown structure and created detailed work packages and cost/schedule baselines. But a usable report format still was not available. Users needed an EVMS output (reporting system) that could operate with a simplified EV data set and

yet was both informative and intuitive. Complexity would be increased over time to meet the users' more complex reporting needs.

The consensus format, developed by July 2005, is a graph that tracks two common project-management information system outputs, the cost performance index (CPI) and schedule performance index (SPI), for each major section of LANL's Nuclear Weapons Program and for the program portfolio as a whole. For example, the new EVMS assesses CPI and SPI data—information vital to managers. The SPI also shows how quickly the programs recovered from the Laboratory's 2004 suspension of work. Although only 64% of work planned for August 2004 could be accomplished, the same programs completed an extraordinary 95% of their scheduled baselines little more than a year later (September 2005).

Customer response, both internal and extenal to the program, was immediate and positive as reliable CPI and SPI information and accurate at-completion estimates became readily and consistently available. Laboratory decision makers had a precise view into the cost and schedule performance of the work within their purview, and DOE/NNSA recognized that the Laboratory had successfully executed an EVMS, the critical component of a thriving project management initiative. NWJ

Point of contact:
Michael Hatfield, 665-9481, hatfield@lanl.gov

Definitions of Terms

cost performance index (CPI)—Number that indicates task, project, or program cost performance. CPI is derived by dividing cumulative earned-value figures by cumulative actual costs. A CPI of "1.00" is considered perfect with lower numbers indicating poor performance and higher numbers indicating optimum performance.

cost/schedule baseline—Plan for executing a project. Cost baseline indicates planned expenditures. Schedule baseline documents planned durations.

decompose—Break into basic elements.

earned-value management system (EVMS)—Management information system that provides cost and schedule performance data for projects.

portfolio—Collection of projects.

project management—Process of planning, organizing, staffing, directing, and controlling the production of a system with the use of software tools.

schedule performance index (SPI)—Number that indicates task, project, or program schedule performance. SPI is derived by dividing cumulative earned-value figures by cumulative budgeted costs. An SPI of "1.00" is considered perfect with lower numbers indicating poor performance and higher numbers indicating optimum performance.

work breakdown structure—Hierarchical list of project outputs.

work package—Piece of a decomposed project; describes the planned resources, time, and output of project work.

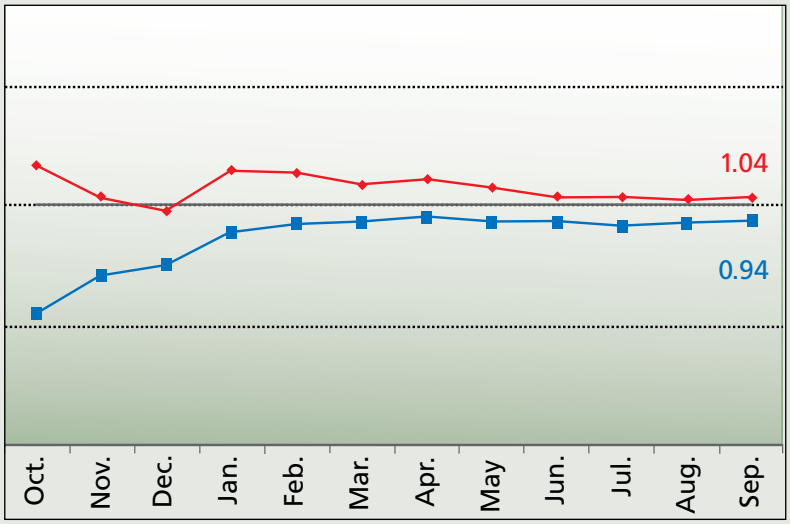

Sample CPI/SPI chart. The CPI (red line) and the SPI (blue line) compare the cost of work accomplished with the cost of work planned for the same time period. This example shows that in a fiscal year, a hypothetical project accomplished $1.04 worth of work for every dollar spent in that year, but the project accomplished only $0.94 worth of work for every dollar allocated for that year. Project management techniques such as this have proved so effective in the industries in which they have been introduced that the federal government now requires their application in almost all large government projects, especially those that involve national defense.

Modeling Permeability Development in Thermally Damaged PBX 9501

The abnormal thermal environments that could lead to ignition of a nuclear weapon high explosive (HE) are of particular concern to LANL scientists charged with stewarding the nation's stockpile.

Postignition response behaviors such as reaction propagation (successive consumption of the explosive) and progression to violent reaction (explosion or detonation) are thought to depend on the explosive's preignition thermal damage state. Thus, accurate response prediction hinges on scientists' ability to calculate the extent to which preignition heat could damage the explosive.

Many factors influence the preignition thermal damage state of PBX 9501, an HE commonly used in nuclear weapons. These factors include heat transfer through the explosive container (a weapon or a test vessel) and chemical reactions within the explosive. In addition, the flow of gas originating from chemical decomposition of the explosive can significantly impact HE response to abnormal thermal environments. For example, LANL researchers have observed complete quenching of violent reaction when a sufficient amount of gas leaks out of the explosive container. At the other extreme, detonation or near-detonation may result in sealed explosive charges that are homogenized (i.e., made highly uniform) by gas flow and heat conduction.

Gas Flow Modeling

Gas flow is important in modeling and simulation studies because weapons systems containing PBX 9501 generally are not spatially uniform when they are subjected to fire. Faster heating on the side of a weapon that is closer to the fire leads to nonuniformity (solid HE decomposes at a higher rate on the hotter side of the weapon). Pressure building in this more-rapidly decomposing explosive continually drives decomposition gas throughout the sealed explosive charge. The presence of decomposition gas accelerates subsequent solid HE reactions. The overall effect of gas flow can be to spread chemical reactivity from the most rapidly decomposing

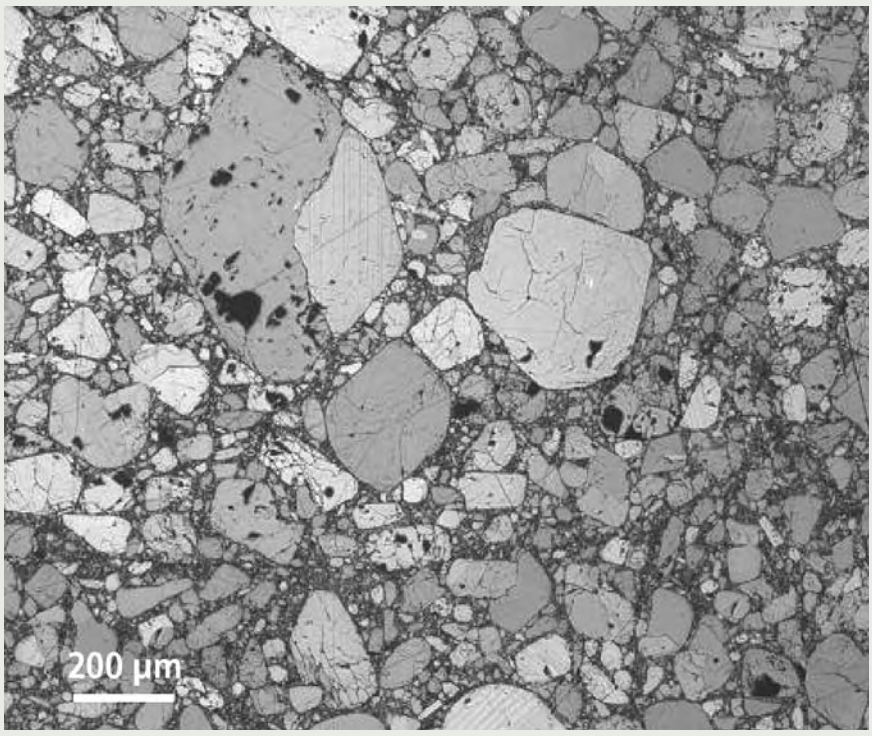

Micrograph of pristine PBX 9501. The larger structures are HMX (an HE) crystals, which are coated with binder that holds the crystals together and decreases the impact sensitivity of PBX 9501. The binder material, a 50:50 mixture of Estane 5703 and nitroplasticizer, makes up 5% by weight of the composite PBX 9501.

Because the binder coats the crystals, it forms a continuously connected 3-D field. The loss of solid mass in the binder facilitates the generation of a microscopic network of porosity, which can be calculated based on the chemical decomposition and solid mass loss of PBX 9501. Through experiments and computer simulation, LANL researchers are improving understanding of the decomposition processes of PBX 9501 by determining the relationship between porosity and permeability development in this commonly used HE.

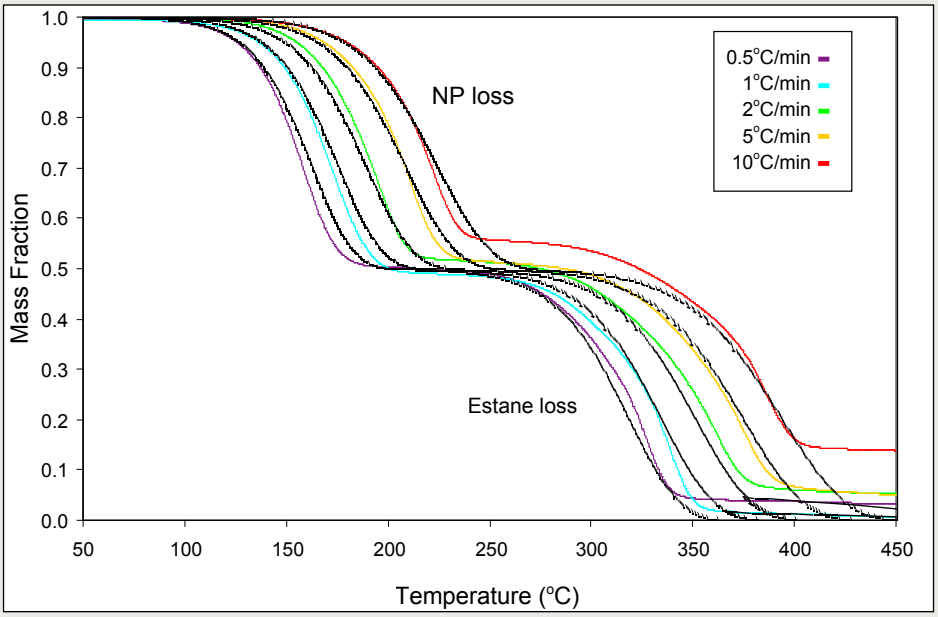

Thermogravimetric data for NP and Estane in a 50:50 mixture by mass (solid lines). Loss of NP solid begins at temperatures below 100°C, although 185°C is sufficient to produce rapid NP loss at all five rates of temperature increase.

In contrast, Estane mass loss does not begin until the temperature exceeds 250°C, with rapid loss better-characterized by a temperature of 325°C.

Black lines show computer simulation results. Kinetic models enable the calculation of porosity generation, i.e., solid mass loss.

side of the explosive to the cooler, less-reactive side. Such explosives tend to become uniform in gas density and overall thermal damage despite their non-uniform thermal environments.

Traditionally, gas flow was not included in modeling and computer simulation of PBX 9501 thermal response due to computational limitations and the lack of permeability data. However, recent advances at LANL now permit gas flow modeling in damaged HE. Research indicates that gas flow can significantly affect the results of calculations used to determine the preignition thermal damage state of PBX 9501.

Gas Transport Modeling

Gas transport in PBX 9501 is readily modeled as flow through a porous medium. Darcy's law provides an appropriate and convenient expression for the area-averaged gas velocity as a function of local pressure gradient, gas viscosity (μ), and permeability (κ) of the porous medium:

$$v_{sf} = \frac{-\kappa}{\mu} \nabla P \ .$$

The permeability of thermally damaged PBX 9501 was unknown prior to experiments performed at LANL in the past several years. These measurements give the increase in permeability of a small sample of HE held at elevated temperature for many hours. To enable the use of Darcy's law in computer simulations, permeability must be a known function of calculated local conditions within the damaged PBX 9501. Locally, permeability is dependent upon the degree of porosity and the development of microscopic gas-flow pathways connecting these pores within the PBX 9501.

Our technical goal is to develop models for calculating interconnected porosity and then relate this porosity to measured permeability. Porosity can be calculated based on chemical decomposition and solid mass loss of PBX 9501, which is approximately 95% by weight HMX explosive, 2.5% nitroplasticizer (NP), 2.5% Estane 5703, and a very small amount of antioxidant stabilizer. NP and Estane make up the binder that coats the HMX crystals, holding them together and decreasing the sensitivity of PBX 9501 to impact.

Data from the following three types of chemical decomposition experiments help us model porosity generation and permeability development in thermally damaged PBX 9501.

1. Thermogravimetric analysis (TGA) to measure solid mass loss from NP and Estane. Kinetic models for NP and Estane solid mass loss are fit to these experiments.

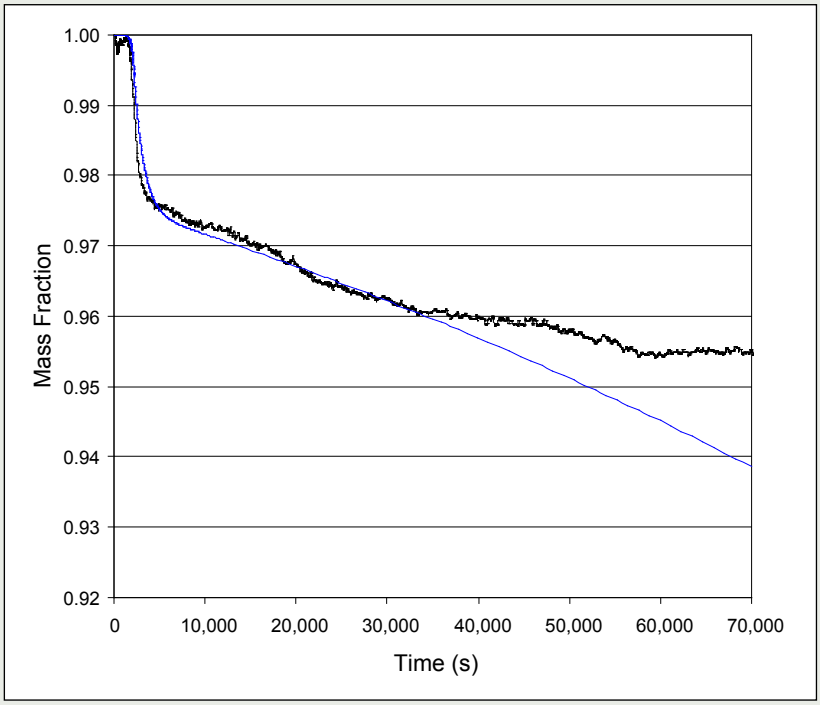

TGA for PBX 9501 at 180°C (black line). A relatively rapid 2.5% solid mass loss occurs in the first hour of the experiment, followed by a much-slower mass loss over the next 18 h.

The blue line shows a computer simulation of this experiment. Early mass loss is modeled as loss of NP from the binder, although the later slow loss is modeled as loss of HMX. Mass loss from both components contributes to the generation of porosity in PBX 9501.

HMX solid mass loss is thought to proceed by a second-order mechanism that corresponds to nucleation and growth. Kinetic parameters for that mechanism were fit to the PBX 9501 TGA data; the binder loss mechanism operated simultaneously.

2. TGA to measure solid mass loss from PBX 9501. Accounting for binder mass loss, a kinetic model for HMX mass loss is fit to this experiment.

3. Permeametry on thermally damaged PBX 9501. Modeling this experiment facilitates correlating porosity with permeability. Note that binder migration is not important in permeability development due to the high viscosity of the molten binder.

The NP and Estane components of the binder are assumed to decompose by a mechanism proposed by scientists at Lawrence Livermore National Laboratory (LLNL). The steps shown in the following table represent NP vaporization, NP vapor combustion, and Estane decomposition to combustion products.

Reaction Mechanism and Thermodynamics for PBX 9501 Binders

Step	Reaction Mechanism	Thermodynamics (J/g)
1	NP(s)[a] → NP(g)[b]	ΔH = +113
2	NP(g) → Products(g)	ΔH = –2937
3	Estane(s) → Products(g)	ΔH = +3975

[a]s = solid
[b]g = gas

Steps 1 and 3 represent solid mass loss and thus porosity generation. These steps were fit with first-order Arrhenius kinetic parameters to the TGA data.

While not contributing directly to porosity generation, the highly exothermic step 2 in the following table also was fit with Arrhenius parameters to match 1-D time-to-explosion data taken at LLNL for Estane and NP.

Arrhenius Reaction Kinetic Parameters for PBX 9501 Binders

Step	Reaction	ln (*A*)	*E* (kJ/mol)
1	NP(s)[a] → NP(g)[b]	14.30	80.0
2	NP(g) → Products(g)	40.43	196.4
3	Estane(s) → Products(g)	16.52	120.5

[a]s = solid
[b]g = gas

A computer simulation using the above reaction mechanism and kinetic parameters shows that binder held at a constant temperature of 185°C for 1 h loses 99% of its NP solid mass but that Estane mass loss is practically zero. Based on these results, the loss of NP solid mass is believed to be responsible for the development of interconnected porosity during PBX 9501 thermal damage events that occur between 150°C and 200°C. Such loss is typical of

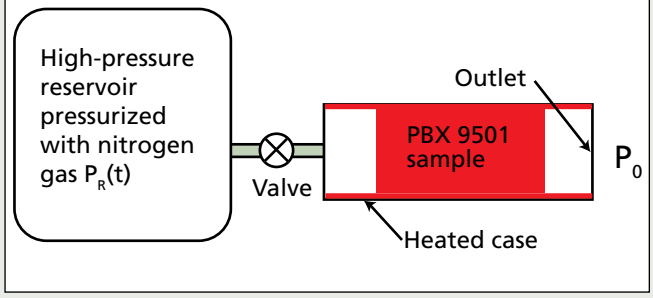

Schematic diagram of PBX 9501 permeameter. Gas in the reservoir is released through the valve and into the heated HE sample. Initial pressure in the reservoir can be as high as 200 psia, with atmospheric pressure (P_0) at the sample outlet. The sample is held at a constant and uniform temperature during the test. $P_R(t)$ is reservoir pressure recorded as a function of time.

abnormal thermal environments that lead to the greatest reaction violence.

PBX 9501 mass loss that is caused by HMX mass loss occurs much more slowly than that caused by NP mass loss. TGA of solid mass loss from PBX 9501 at 180°C shows a rapid loss of 2.5% in the first hour of the test. This change is followed by a much-smaller loss rate, resulting in an additional 2% to 3% solid mass loss over the next 18 h. Presumably the early loss can be attributed to NP and the later loss to HMX. This experiment was modeled using a homogeneous mixture of HMX and binder in the same proportions as in PBX 9501. The loss of binder components was modeled using the mechanism and kinetic parameters in the tables above.

HMX solid mass loss is thought to proceed by a second-order mechanism that corresponds to nucleation and growth. Kinetic parameters for this mechanism were fit to the PBX 9501 TGA data with the binder loss mechanism operating simultaneously.

The HMX mass loss expression corresponding to the second-order mechanism is

$$\dot{R}_{HMX} = -k\rho_{HMX}\left(1-\frac{\rho_{HMX}}{\rho_{PBX_0}}\right),$$

where ρ_{HMX} is the total-volume average density of HMX and ρ_{PBX_0} is the initial total-volume average density of the PBX 9501. The ratio ρ_{HMX}/ρ_{PBX_0} must be less than unity for mass loss to commence in this model and is approximately 0.95 at the beginning of the computer simulation of PBX 9501 TGA data.

The kinetic rate constant, k, has a modified Arrhenius form

$$k = AT\exp\left(\frac{-E}{RT}\right),$$

where T is temperature and R is the universal gas constant. Values for the fitted parameters are $\ln(A) = 22.05$ and $E = 150$ kJ/mol.

Using this mass-loss law, HMX decomposes to gaseous products more slowly than the NP. However, PBX 9501 is nearly 95% HMX by mass, so its slow yet continuous decomposition over many hours leads to a measurable increase in porosity.

Permeability Measurements

Global measurements of permeability provide the final experimental data required to relate porosity to permeability. In those tests, a permeameter designed and built at LANL was used to measure pressure drop as a function of time across a thermally damaged sample of PBX 9501. Initially, the reservoir was pressurized with nitrogen gas. The sample was held at a constant temperature for a specified period of time before the reservoir valve was opened. Reservoir pressure, P_R, was recorded as a function of time. Reservoir pressure decreases more rapidly for samples that have greater permeability.

The experiment was modeled with a computer simulation to fit the measured reservoir pressure transient by manipulating permeability. The simulation included mass conservation equations for NP (solid and gas), HMX, Estane, product gas, and nitrogen. These equations included (1) advection of gaseous species caused by flow and (2) species mass consumption or production caused by chemical reaction. The gases generated within the sample during thermal damage and the nitrogen coming from the reservoir are subject to flow (as described by Darcy's

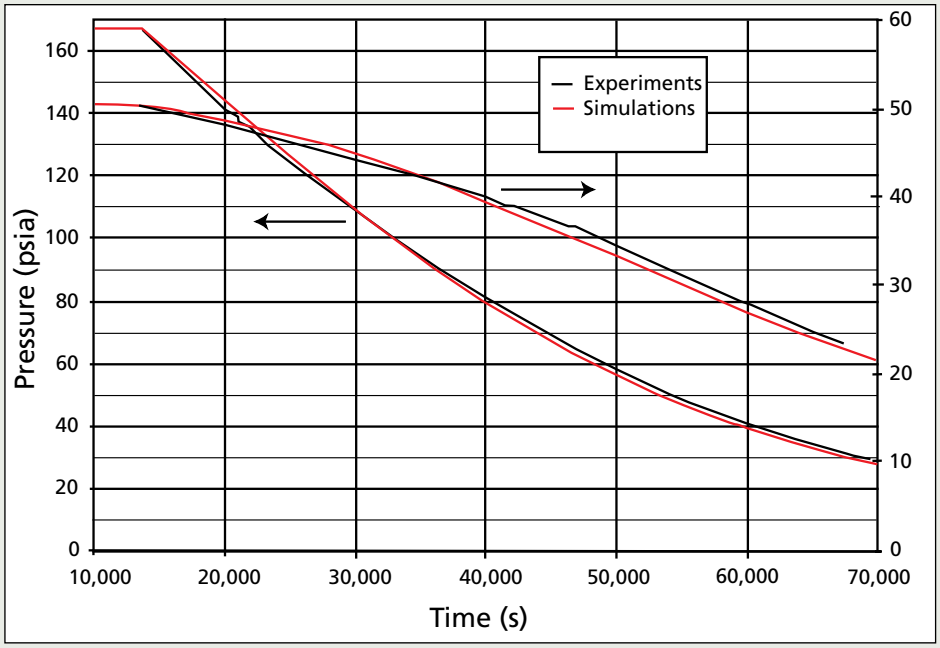

Permeameter reservoir pressure transient. Samples were held at 185°C for approximately 3.5 h before the reservoir valve was opened.

Black lines show data from two experiments. The left-hand axis corresponds to an initial reservoir pressure of 166 psia and the right-hand axis corresponds to an initial reservoir pressure of 50 psia.

Red lines show computer simulation results for the two experiments. The Kozeny-Carmen constant giving the best fit is 1.0 x 10^{-12} m², giving permeability of approximately 1.0 x 10^{-15} m² at the end of both tests.

law). The fitting parameter is K_0, from the Kozeny-Carmen equation relating permeability to porosity in porous media:

$$\kappa = K_0 \frac{\phi^3}{(1-\phi)^2} \cdot$$

Porosity, ϕ, develops over time as the NP and HMX components of PBX 9501 vaporize and decompose. At a temperature of 185°C, the NP is practically gone after 3.5 h, generating approximately 3.4% calculated porosity. The HMX continues to lose solid mass throughout the simulation. The total calculated porosity after 70,000 s is approximately 9% to 10%. With a fitted value for the Kozeny-Carmen constant of K_0 = 1.0 x 10^{-12} m², the calculated permeability of the thermally damaged PBX 9501 at the end of the tests is approximately 1.0 x 10^{-15} m². With this simple relationship, the permeability at any location within thermally damaged PBX 9501 can be calculated from the extent of porosity at that location.

Through strong collaboration across the Laboratory, the LANL Surety Program continues to improve understanding of PBX 9501 decomposition processes and modeling of permeability development. Ongoing Laboratory experiments are disclosing the competing effects of HMX vaporization and direct solid decomposition. Additional permeameter tests are planned that will isolate NP and HMX mass-loss effects and examine the permeation response of PBX 9501 at elevated pressures and decreased pressure gradients.

LANL's Surety Program investigations of mechanisms such as gas flow in thermally damaged PBX 9501 demonstrate the program's commitment to resolving issues that could impact the safety of the nuclear weapons stockpile. NWJ

Points of contact:
Dave Zerkle, 665-3582, dzerkle@lanl.gov
Blaine Asay, 667-3266, bwa@lanl.gov

Other contributors to this article are Gary Parker, Peter Dickson, and Lloyd Davis of the Materials Dynamics Group; Laura Smilowitz and Bryan Henson of the Physical Chemistry and Applied Spectroscopy Group; Larry Luck of the Nuclear Design and Risk Analysis Group; and Craig Tarver, LLNL.

Trident Tests Dynamic Response of Plutonium

Understanding the dynamic response of special nuclear materials, particularly of plutonium, is fundamental to predicting the performance of nuclear weapons. As stewards of the nuclear stockpile, LANL scientists must collect data on the dynamics of modern weapons materials to ensure long-term reliability without rebuilding plutonium weapons pits.

Because of the hazardous nature of the material and because the dynamic behavior of plutonium is much more complicated than that of most other metals, collecting dynamic plutonium data safely can be difficult and costly. Interpreting experimental results is seldom straightforward and may not be consistent with expected outcomes.

To help explain and quantify specific dynamic behaviors of plutonium, a group of scientists from across the Laboratory have conducted collaborative research on the spall strength and possible phase transitions of plutonium. Our cooperative work culminated in September 2005 with four innovative experiments at LANL's Trident laser laboratory.

Using two optical interferometers (a point VISAR and a line-imaging interferometer) during each experiment, we recorded the free-surface velocity of each sample after a gold laser-launched flyer plate impacted the sample. Interferometers are optical instruments that record the position and/or change in the angle of an optical signal reflected from a surface and convert the signal to velocity—in this case the velocity of the unconfined plutonium surface, sometimes called the free surface.

Trident tests achieve definitive results safely and cost-effectively.

Trident is primarily used at pulse lengths of a few nanoseconds for inertial confinement fusion experiments and for diagnostics development for the National Ignition Facility. However, Trident also can generate long pulses of up to several microseconds and deliver 400 to 500 J/pulse. Using Trident in the long-pulse mode and a confined plasma ablation mechanism, we can accelerate flyer plates without generating significant shocks in the accelerated plates.

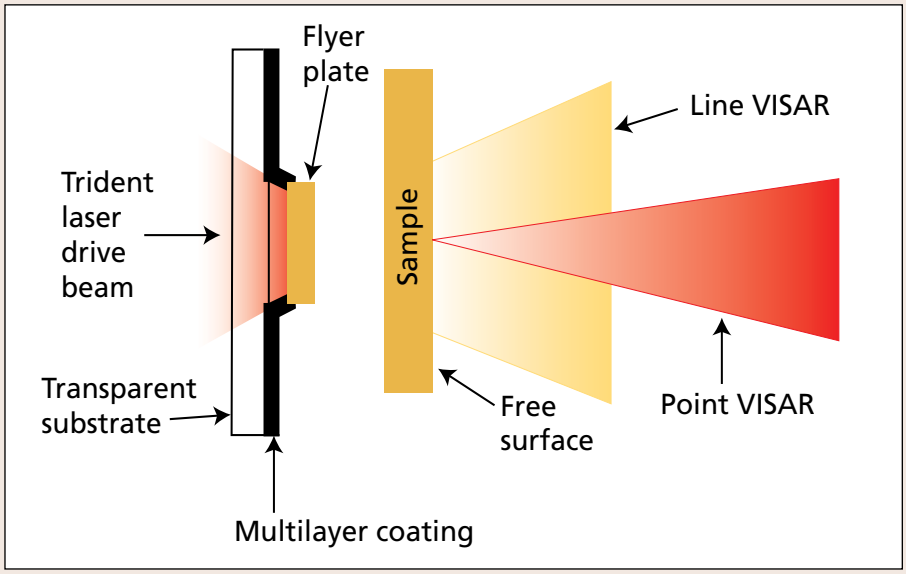

Side view of experiment setup. The Trident laser beam is pulsed through a transparent substrate, depositing the laser energy between the substrate and the flyer plate.

The high-pressure plasma accelerates the flyer plate away from the substrate and into (i.e., the plate impacts) the plutonium target (sample). Almost no ancillary experiment material impacts the target material, which minimizes collateral damage to the target and its environment and makes containment, recovery, and postexperiment metallurgical analysis possible.

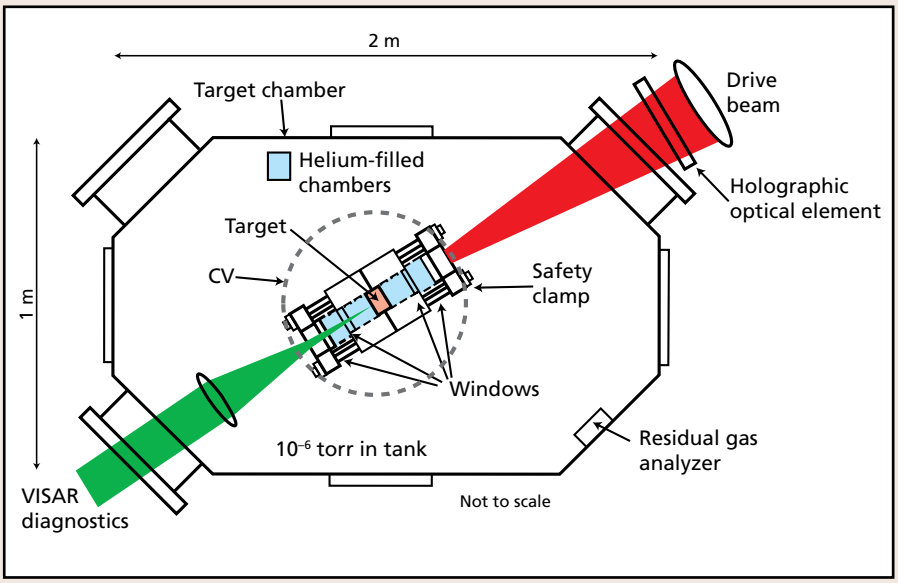

Top view of experiment setup. A containment vessel (CV), plutonium target (sample), and flyer plate are placed inside a Trident glovebox-like target chamber. The CV is backfilled with 1 atm helium and continuously monitored for helium leaks (which would indicate failure of the CV safety envelope). A Trident drive beam launches the flyer plate. Optical interferometers monitor the free-surface velocity profile of the impacted plutonium sample.

This test series was conducted on four plutonium control samples. The samples were from the Accelerated Aging of Plutonium Project, which supported the Laboratory's Enhanced Surveillance Campaign.

Laser-Launched Flyer Plates

The confined plasma-ablation method was developed for launching thin (2- to 20-μm) flyer plates to initiate shock in explosives.

However, with Trident's increased laser pulse length and energy, our research group has launched thicker flyer plates from several hundred meters per second to as fast as ≥3 km/s. These plates were 0.2 to 2 mm thick and 8 mm in diameter and were composed of many different metals (gold, tantalum, tungsten, aluminum, tin, or copper). Because the flyer plates and targets (samples) can be many times the material's grain size and therefore represent a bulk material response, the results of our experiments represent the metal's bulk property response. Thinner laser flyer plates can be used to shock single grains and grain boundaries to study individual properties that in total may represent bulk response.

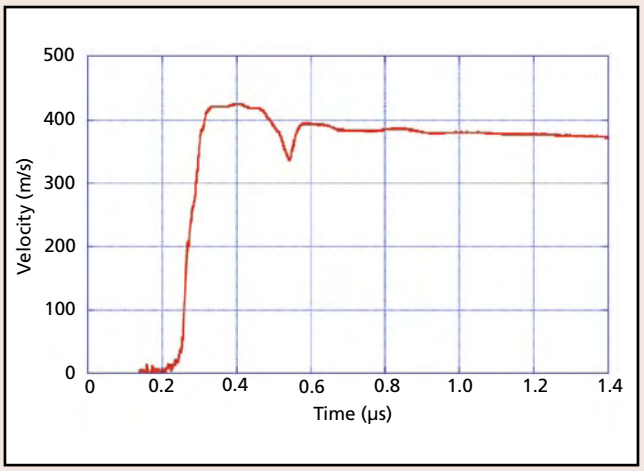

Spall experiment using high-purity tin. Spall strength is quantified by recording the free-surface velocity of the target material (sample). Using the rate of the reduced velocity (from 420 to 330 m/s), the return velocity (back from 330 to 390 m/s), and known properties of the material, the dynamic spall strength and the strain rate of the material can be determined. These data are from an experiment with a tin sample, but are typical of data for many materials.

Trident-launched flyer plates are smaller than those accelerated by more conventional methods such as gas guns and explosive plane-wave lenses. Laser flyer plates also produce much less collateral damage inside the evacuated target chamber than usually results from the explosives or sabots required for gas guns. None of these experiments produces collateral damage outside its safely enclosed test environments. The smaller size and the reduced collateral damage that are characteristic of the laser-launched plates

- permit the use of smaller sample size,
- use somewhat less-costly equipment,
- increase the possibility of reusing normally expended hardware and equipment,
- reduce experiment setup time,
- virtually eliminate potential contamination in the testing environment, and

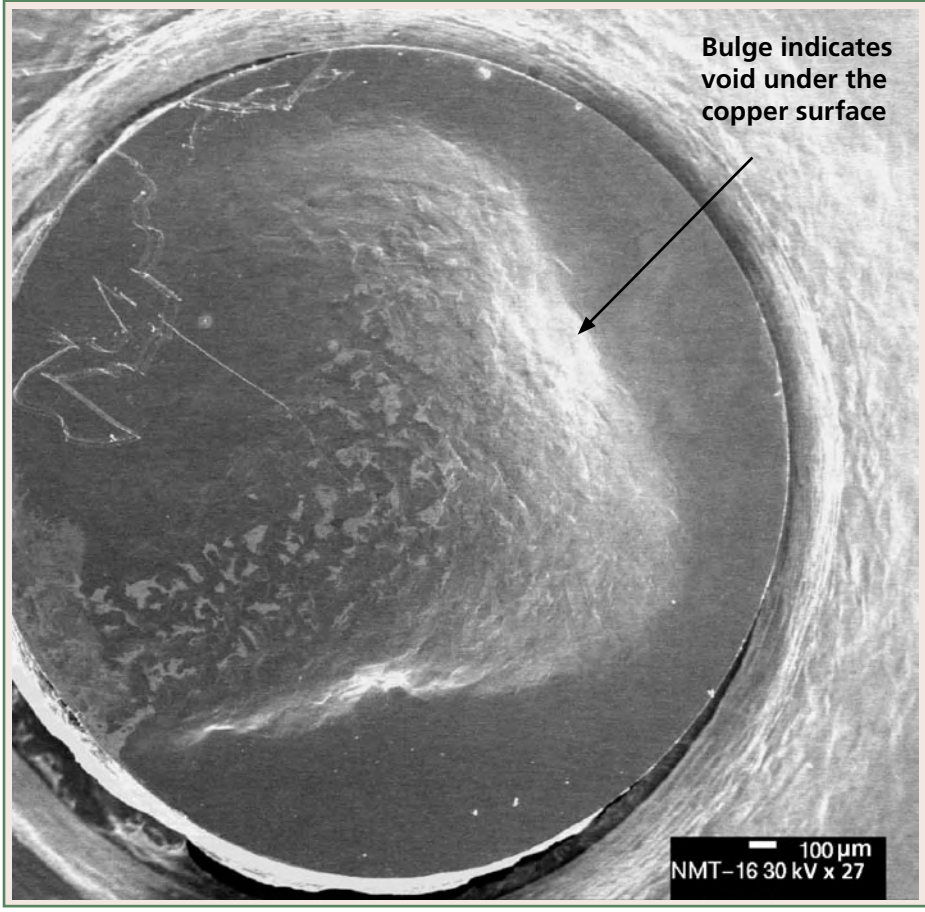

Effects of extreme tensile stress. The incipient spall of this copper sample indicates how a metal will separate internally when its tensile stress is greater than its spall strength.

In this experiment, a 5-mm-diameter sample is held tightly inside a 10-mm-diameter ring of the same copper. The smooth (+/–100 nm) surface of the sample is impacted on its opposite side by a copper flyer plate; the impact generates a shock wave in the sample.

Shock waves reflected from the surface of the sample and from the flyer plate create intersecting release waves (tensile waves of negative pressure) that cause the sample to mechanically fail in tension, which creates an irregular open pocket (void) that is approximately 3 mm in diameter.

- make containment and full sample recovery much easier and safer than most other experiment methods.

For our Trident experiments, each sample was placed in a small target holder with an accompanying flyer plate attached to a transparent sapphire substrate. Each flyer/target assembly was placed inside a hermetically sealed containment vessel (CV). Each CV had four optical windows: two for entry of the Trident laser drive beam (to launch the flyer plate) and two for diagnostic lasers (so that interferometers could record the response of the plutonium sample at impact). At the same time, streak cameras and digitizers recorded the dynamic experimental data to provide further data-comparison and data-backup systems.

The CVs fully contained all plutonium samples before, during, and after each experiment. The-sealed, as-tested CVs were returned to Nuclear Materials Technology Division's Nuclear Materials Science Group (NMT-16) at the Chemistry and Metallurgy Research Building for full sample removal.

Test Results

NMT-16 is conducting metallographic analyses of the recovered targets to correlate the dynamic response data we collected in these four Trident shots. However, preliminary data analysis suggests that our results are consistent with other plutonium dynamic experimental methods.

The data also presented several new dynamic observations that will require further study. These data and metallography results will be shared with Laboratory modelers to help guide code development for weapons material dynamics.

Our Trident laser experiments are not only technically successful, they are extremely cost-effective.

First, completing this set of four plutonium experiments in three shot days demonstrated that LANL has developed the ability to conduct suc-

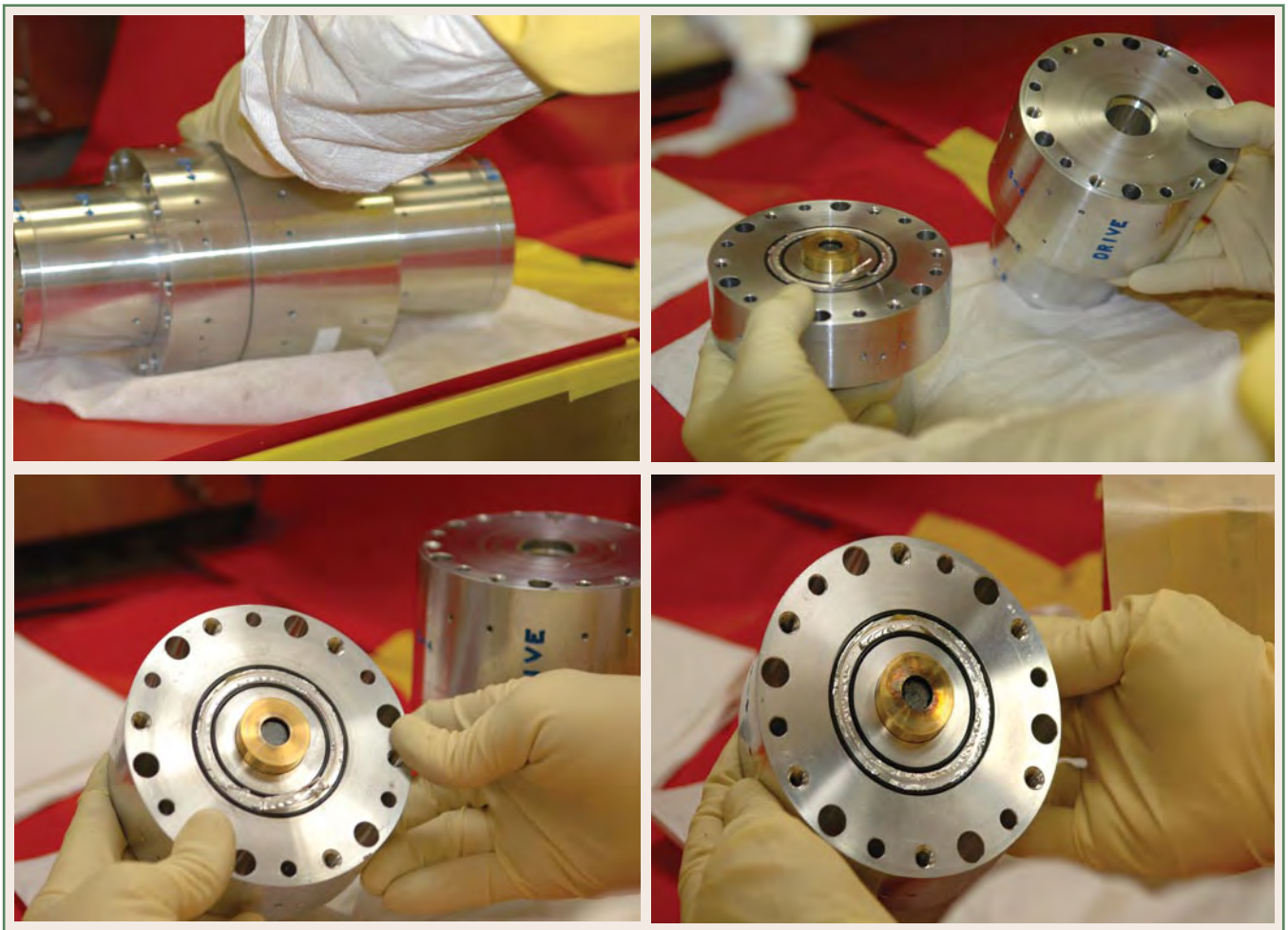

CV after shot. A radiological control technician receives the CV that encapsulates the flyer plate and plutonium target (sample) (*top left*). Separating the two parts of the CV reveals the plate and sample, which were inserted in a brass and aluminum housing before the shot (*top right*). A triple containment system (O-rings, indium seals, and two windows) prevents the accidental release of plutonium from the CV; prohibits the spread of contamination throughout the assembly, disassembly, and experiment processes; and allows safe, easy recovery of the target. The two black rings are the rubber O-rings; shiny, rough material is the indium seal (*bottom left*). Smudges on the brass indicate condensed plasma matter deposited from the laser on the substrate (*bottom right*).

cessful experiments with rapid turnaround time (potentially up to four shots per day). Conducting multiple shots per day reduces equipment and personnel setup time as well as some equipment expenditures usually associated with traditional experiment methods.

Second, the CV fully encapsulates the plutonium sample, which eliminates contamination to personnel and equipment and in many cases allows equipment reuse, significantly reducing many of the safety and equipment costs of critical weapons research. NWJ

Points of contact:
Dennis L. Paisley, 667-7837, dxp@lanl.gov
Carter P. Munson, 667-7509, cmunson@lanl.gov

Other contributors to this research include Thomas E. Tierney and Billy Vigil of the Hydrodynamics and X-Ray Physics Group; Davis Tonks of the Applied Science and Methods Development Group; Dan Schwartz and Mike Ramos of the Nuclear Materials Science Group; Luis Morales and Tom Zocco of the Enhanced Surveillance Campaign; Tom Sedillo, John Jimerson, and Sam Letzring of the Plasma Physics Group; Ron Snow and Ron Perea of the Polymers and Coatings Group; Roberta Mulford of the Pit Disposition Science and Technology Group; Kenneth Ault of the RO Operations Group; and the long-term collaborative work of many individuals and groups, including the Trident laser staff.

National Security Sciences Building

The 275,000-square-foot National Security Sciences Building (NSSB) was dedicated May 20, 2006, at the celebration of the University of California's 63 years of service to the nation as the manager of the Laboratory. Senator Pete Domenici officiated at the ribbon-cutting ceremony. NNSA Administrator Linton Brooks, New Mexico Governor Bill Richardson, and Laboratory Director Bob Kuckuck also spoke at the dedication.

The NSSB replaces the Administration Building, a more than 50-year-old structure, at Technical Area 3. At a later date, the Administration Building will be decommissioned and decontaminated in preparation for demolition.

A memorial to the victims of the September 11, 2001, terrorist attack was also dedicated during the NSSB dedication ceremonies. Located near the entrance to the new building, a piece of limestone salvaged from the damaged part of the Pentagon is mounted on a welded stainless steel frame made by the KBR-SHAW-LATA Nevada Test Site shop and inscribed with the names of the 184 people who died during the attack on that building.

The building is designed to house approximately 700 staff members in 680 offices. Additionally, the NSSB has 17 conference rooms that, if all were occupied at the same time, could hold a total of approximately 500 employees.

LANL personnel will occupy seven of the eight stories of the NSSB. On the first floor a 600-seat lecture hall and auditorium can accommodate hearing- and mobility-impaired employees. Floors two through seven are offices and conference rooms. The eighth floor is a mechanical and equipment room. LANL personnel began moving into the NSSB on May 31st.

The NSSB also contains a 26,000-square-foot records storage facility. It is the only records storage facility in New Mexico that is certified by the National Archives Record Administration and one of only two certified records storage areas in the entire DOE Complex.

As part of the $97 million NSSB project, a 400-space parking garage was constructed directly north of the Oppenheimer Study Center. Construction began on the parking garage in May 2004 and it opened in May 2005. NWJ

Quasi-Static and Shock Compressive Response of Kel-F 800

Widely used in a variety of engineering applications, fluoropolymers are attractive research materials because they are chemically inert, have a low coefficient of friction, and tolerate high-temperature operating conditions. Their inherently high densities also make them extremely desirable as high explosives binders, particularly in insensitive plastic-bonded explosives (PBXs).

PBX 9502 and LX-17 are two modern insensitive (i.e., less-easily initiated) PBXs whose polymeric binder is poly(chlorotrifluoroethylene-*co*-vinylidene fluoride), commonly known as Kel-F 800.

The dynamic compressive behavior of a PBX is likely influenced by the response of its polymeric binder, particularly under low-pressure conditions. Although Kel-F 800 has been used as a polymeric binder in weapons for many years, LANL scientists are the first to investigate the shock wave and quasi-static compressive responses of this material. Using 1-D plate impact experiments, LANL researchers have now established a baseline Hugoniot (locus of shocked states) equation of state for two well-characterized Kel-F 800 sample materials, examined the role of crystallinity on the compressive properties of this widely used PBX binder, and conducted hydrostatic compression pressure-volume-temperature tests. The investigation of the influence of crystallinity is particularly important in this work because crystallinity in polymers can act as a physical cross-link, stiffening the polymer network.

Sample Preparation

Two sample-preparation methods were used to create small cylindrical billets of solid polymer from Kel-F 800 pellets. In the first method, the pellets were compression-molded (CM); i.e., the pellets were heated to 90°C and pressed at approximately 50,000 psi. This method produced an off-white material with opaque white particles dispersed throughout. Differential scanning calorimetry (DSC) revealed evidence of incomplete pellet melting in the billets, and the presence of water contained in the opaque white particles.

At low shock pressures, Kel-F 800 is softer than Kel-F 81 or PVDF. Under quasi-static conditions, compression-molded material is slightly softer than melt-processed Kel-F 800.

In the second method, the pellets were melt-processed (MP); i.e., the pellets were heated in Pyrex beakers to 110°C to 120°C and cycled periodically between vacuum and ambient conditions. After several days, the MP method achieved a material that was optically transparent and amber in color; it contained no inclusions (particles).

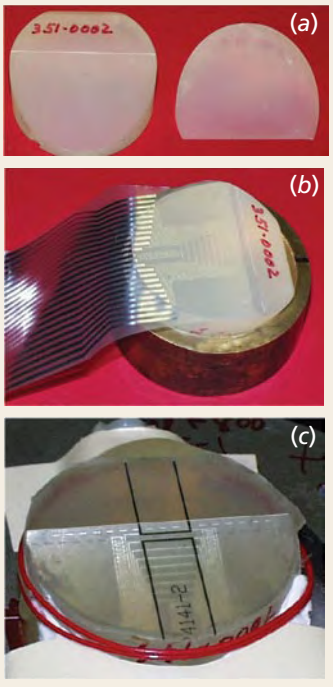

Kel-F 800 target. Targets were prepared by machining the solid polymer Kel-F 800 into cylinders, cutting the cylinders at a 30-degree angle (*a*) to insert a gauge membrane (*b*), and affixing a stirrup gauge to the target impact face (*c*).

The embedded electromagnetic gauges in the membrane measure shock wave profiles in situ and are used to extract shock and particle velocities and sound velocities at pressure.

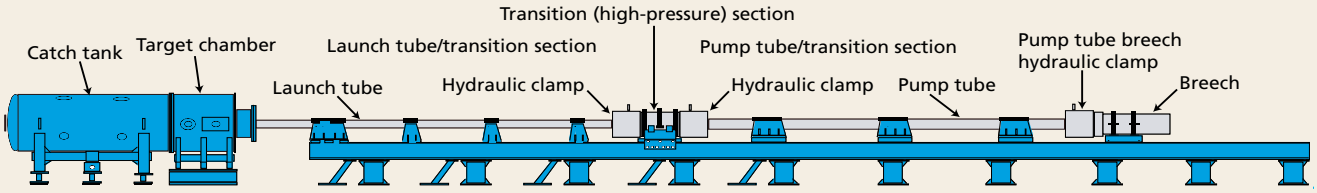

Gas gun experiment. Used to characterize the shock dynamics and behavior of many types of materials included in the nuclear stockpile, a gas gun measures and records events that occur in microseconds. A piston accelerated by gas pressure contained in the breech end of the gun forces the helium in the pump tube to be compressed and raises the pressure until a calibrated disk (burst diaphragm) opens and forces the gas toward the launch tube. Pressure from that gas accelerates a projectile down the launch tube and into the Kel F-800 target. A catch tank fully contains (catches) debris created by the impact. Embedded (in situ) electromagnetic gauges are the primary diagnostic used to measure shock and particle velocity in the experiment.

Kel-F 800 sample preparation. Granular starting material (Kel-F 800 pellets) (*a*) was heated to prepare cylindrical billets of solid polymer.

Samples prepared by CM at 90°C and approximately 50,000 psi retained opaque white particles that contain entrapped water (*b*).

MP samples, heated in glass beakers at 110°C to 120°C and cycled between ambient and vacuum several times (*c*), are slightly darker, less dense, and less crystalline than CM-prepared samples.

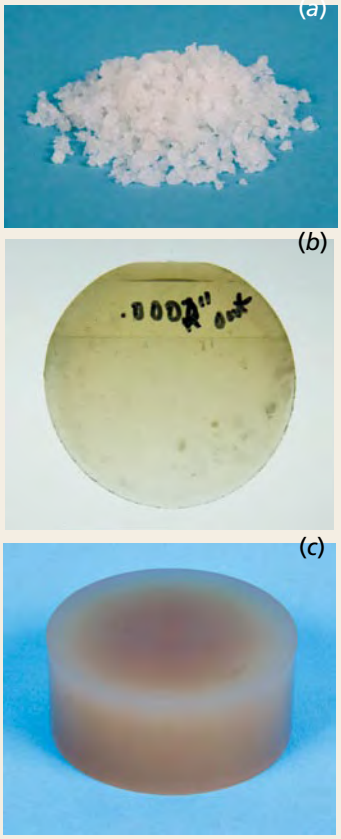

Several analytical methods were used to characterize the materials used in the studies, including thermal analysis using DSC, density measurements by immersion, and gas (helium) pycnometry.

Test Methods

Pressure-volume-temperature measurements were performed using a piston-cylinder apparatus at Datapoint Laboratories; pressure-volume measurements were made at 0, 40, 80, 120, 180, and 200 MPa at 33°C.

Plate impact experiments were conducted on CM- and MP-prepared targets using both single- and two-stage light gas (e.g., helium) guns. Sapphire or other single crystal materials were used for single-stage gas gun impactors. Kel-F 81, which is poly-(chlorotrifluoroethylene), one component of Kel-F 800, was used for the two-stage gas gun impactors. All impactors were contained in Lexan projectiles and launched at Kel-F 800 targets. The targets were prepared by machining the solid polymer (Kel-F 800) pieces into cylinders, cutting the cylinders at a 30-degree angle to insert the gauge membranes, and affixing a stirrup gauge to the target impact face. Electromagnetic gauges are frequently used to study shock-to-detonation processes in high explosives at LANL.

Results

Using DSC, researchers determined that CM-produced Kel-F 800 has (1) a glass transition temperature (i.e., the temperature at which a polymer transitions from glassy to rubbery and is associated with the polymer's amorphous content) of 30.1°C and (2) a multifeatured melt transition (maxima at 78°C and 106°C). The transition at 106°C most likely results from incomplete melting of the crystalline pellets during processing. The opaque particles in the CM material, also found by DSC and thermogravimetric analysis coupled with mass spectrometry, were entrained water that resulted from the processing procedures. The CM material has a density of approximately 2.028 g/cm^3 and crystallinity of 10% to 15% by DSC (integration under melt endotherm, also known as heat of fusion).

Kel-F 800 billet material obtained by MP is slightly darker in color with a glass transition temperature of 25.9°C and a single melt transition at 77.9°C; it also is less dense (1.990 g/cm³) and less crystalline (0.7% to 1.3%) than CM-produced Kel-F 800. There was no evidence of loss of molecular weight of the MP polymer, and the slight darkening of the material that occurred during processing is likely related to the presence of up to 2% emulsifiers and impurities.

The results of five Kel-F 800 plate impact experiments are shown in the table below. Shock (U_s) and particle (u_p) velocities were derived from the response of the embedded electromagnetic gauges; the stirrup gauge response was also used to determine particle velocity. A voltage rise associated with each gauge is proportional to particle velocity in the material, the magnetic field strength, and gauge length. Shock-wave pressures for the experiments varied from 3.0 to 15.4 GPa.

Typically, shock data can be fit to the linear Rankine-Hugoniot equation $U_s = c_0 + su_p$. For CM Kel-F 800, $U_s = c_0 + su_p$ gives $s = 1.855$ (±0.054) and $c_0 = 1.809$ (±0.059) mm/μs. A fit to all the data points gives similar results, with $s = 1.824$ (±0.052) and $c_0 = 1.838$ (±0.059) mm/μs. These values fall within the error of the fit to the CM Kel-F 800, indicating that the two materials behave similarly.

On lower-velocity experiments, the Lagrangian sound velocity at pressure was also extracted from the transit time of the rarefaction wave as a function of gauge depth on the embedded electromagnetic gauges. Sound velocities at pressure are shown in the rightmost column of the table.

Results of the isothermal quasi-static pressure-volume-temperature measurements reveal that the extrapolated zero-pressure isothermal bulk moduli of the two materials differ slightly with the CM material being slightly softer.

Observations

This LANL study is the first to identify the shock response of Kel-F 800, the high explosive binder in insensitive high explosives PBXs. The study also examined both the dynamic and quasi-static compressive response of Kel-F 800 as a function of crystallinity. Observations resulting from the study include the following.

- At low shock pressures, Kel-F 800 is softer than either Kel-F 81 or polyvinylidene fluoride (PVDF), two related fluoropolymers, and the polymer's monomeric constituents. Under quasi-static conditions, the compression-molded material is slightly softer than the melt-processed material.

Kel-F 800 Plate Impact Experiments

Projectile velocity (mm/μs)	Material	Impactor	Density (g/cm³)	U_s (mm/μs)	u_p (mm/μs)	Pressure (GPa)	c_L (mm/μs)
0.63	CM	Sapphire	2.028	2.822	0.531	3.0	4.7
1.12	CM	Sapphire	2.029	3.260	0.737	4.9	5.8
2.00	MP	Kel-F 81	1.980	3.745	1.009	7.5	*
2.72	MP	Kel-F 81	1.990	4.296	1.368	11.7	*
3.19	CM	Kel-F 81	2.027	4.860	1.567	15.4	*

C_L = Langrangian sound velocity at pressure
* = no data

- CM- and MP-prepared Kel-F 800 behave similarly under shock compression, even with a crystallinity difference of approximately 10% to 15% and a density difference of approximately 2%.

- Static isothermal data indicate considerable network or free volume in the polymer network, compared with other linear fluoropolymers, such as poly(tetrafluoroethylene).

Related LANL studies will further investigate

- the influence of specific polymer features (such as crystallinity) on the compressive response of this widely used polymer;

- Kel-F 800 crystalline phase transitions, rate-dependent viscoelastic response, and isentropic compression behavior; and

- the dynamic (shock) response of Kel-F 800 material that is representative of material in the pressed PBX.

Information from these studies will be used to formulate realistic, physics-based equations of state and constitutive models for Kel-F 800 and its composites (i.e., PBX 9502). NWJ

Points of contact:
Dana Dattelbaum, 667-7329, danadat@lanl.gov
Stephen Sheffield, 665-0350, ssheffield@lanl.gov

Other contributors to this article are David Robbins, Richard Gustavsen, Robert Alcon, Joseph Lloyd, and Pete Chavez of the Shock and Detonation Physics Group; Edward Orler of the Polymers and Coatings Group; Ralph Menikoff of the Explosives and Organic Materials Group; Datapoint Laboratories (Ithaca, NY); Larry Hatler and coworkers of the Weapons Engineering Group; Brad Clements of the Equation of State and Mechanics of Materials Group; and members of the Polymers Under Dynamic Loading Team funded by the DOE/DoD Joint Munitions Program.

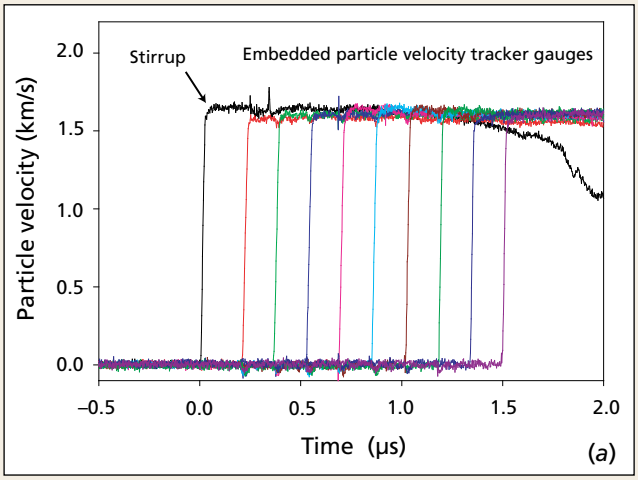

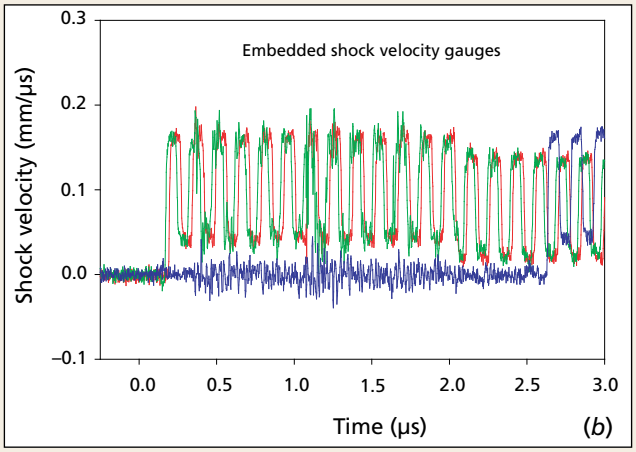

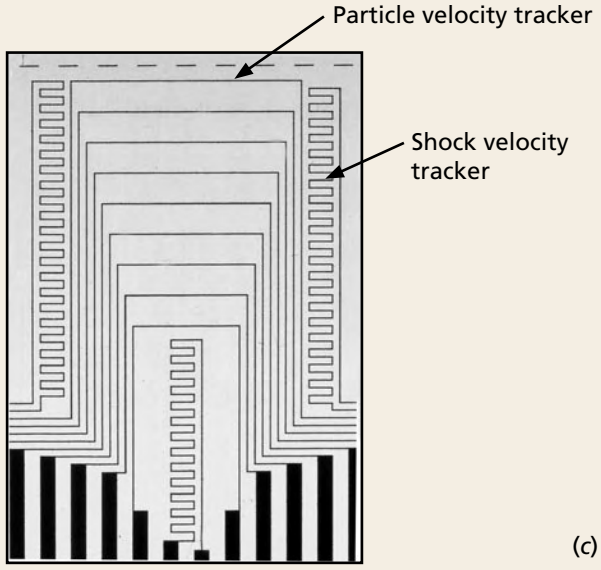

Typical Kel-F 800 dynamic wave profiles as a function of time and position. Shock velocities were calculated using the arrival times of the shock waves at nine particle velocity gauges (*a*) and three embedded shock gauges (*b*) with pressure at 15.44 GPa. Particle and shock velocity trackers (*c*) were embedded in the membrane, which was embedded in the target.

Carbon Monoxide Poisoning

What is colorless, odorless, and can kill? One answer is carbon monoxide (CO).

CO is a gas that is produced when a fuel does not burn completely. Fuels commonly used in the home are wood and charcoal and fossil fuels such as natural gas, oil, coal, gasoline, and propane.

Any fuel-burning appliance in your home is a potential source of CO. Some fuel-burning appliances are stoves, gas dryers, water heaters, and heating units. Burning charcoal or running a generator in an attached garage, basement, crawlspace, or living area of the home can produce dangerous levels of CO. Running a car in the garage, even with the garage door open, can produce a fatal amount of CO in the home.

The Centers for Disease Control analyzed 2001–2003 data on patient visits to emergency departments and 2001–2002 death certificate data from the National Vital Statistics System (*Journal of the American Medical Association* **293,** 1183–1186 [2005]). These statistics are all based on non-fire-related incidents; i.e., CO that was produced by some means other than a fire. The following are some of those statistics:

- during 2001–2002 an average of 480 persons died annually from CO poisoning
- during 2001–2003 an average of 15,200 persons were treated for unintentional CO exposure
- males were 2.3 times more likely than females to die from CO poisoning
- adults over the age of 65 account for approximately 24% of CO poisoning deaths
- approximately 64% of the nonfatal CO exposures occurred in homes
- the highest numbers of fatalities occurred in December and January
- faulty furnaces caused 18.5% of CO exposure incidents
- motor vehicles caused 9% of CO exposure incidents.

The initial symptoms of CO poisoning include headache, fatigue, shortness of breath, nausea, dizziness, or unusually red cheeks. You might feel as if you have the flu, but without the fever. If you suspect that you have CO poisoning, exit the home and get fresh air immediately. If you do not get fresh air, you could lose consciousness and die. Get medical attention as soon as possible and tell medical personnel that you suspect CO poisoning.

Some obvious indications that CO may be present in your home are:

- rusting or water streaking on a vent or chimney
- loose or missing furnace panel
- debris or soot falling from chimney, vent, fireplace, or appliance
- loose or disconnected vent, chimney, fireplace, or appliance
- loose masonry on a chimney
- moisture inside windows.

Some hidden indications that CO may be present in your home are:

- internal appliance damage or malfunctioning components

- improper burner adjustments
- blockage or damage in chimneys
- CO poisoning symptoms are experienced at home, but lessen or disappear when you are away from home.

Only a trained technician can detect and repair hidden problems.

What should you do to help prevent CO poisoning? To protect you and your family, install battery-operated or plug-in CO alarms with battery backup in the hallway near the bedrooms in each sleeping area. If you work on vehicles or use anything that could produce CO, install a CO alarm in the garage or workshop. The US Consumer Product Safety Commission recommends consumers install CO detectors that meet requirements of the Underwriter's Laboratories voluntary standard 2034. This standard requires detectors to sound an alarm when CO reaches hazardous levels. Replace batteries and test the units frequently.

Proper installation, upkeep, and use of CO-producing appliances is the best way to reduce the risk of CO poisoning. Make sure that appliances are installed according to the manufacturer's instructions and local codes. It is best to have appliances installed by professionals. Follow the manufacturer's instructions for operation and make sure that the appliance is used only for its intended use. Have the heating system, including chimneys and vents, inspected annually by a trained technician. Examine vents and chimneys for improper connections, stains or rust, and visible cracks. Look for problems that indicate an appliance is operating improperly: decreased hot water supply, a furnace that runs continuously or cannot heat the house, soot on or under appliances or vents, an unfamiliar or burning odor, and increased moisture inside the windows. Opening doors and windows or using fans will not prevent CO buildup.

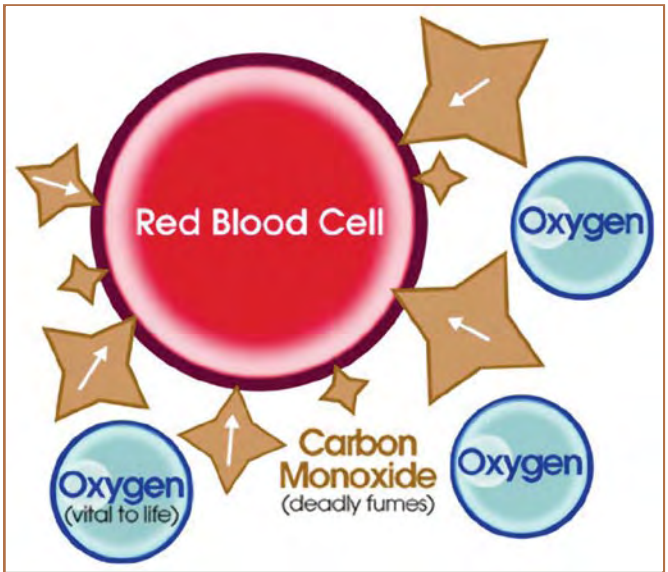

CO displaces oxygen from the bloodstream (thus the red cheeks).

Everyone should follow these warnings regarding CO:

- never leave a car running in the garage
- never leave a generator running in the garage, home, or crawlspace
- never burn charcoal in a tent, home, vehicle, or garage
- never install or service a combustion appliance without proper knowledge, skills, and tools
- never use a gas oven or range for home heating
- never put aluminum foil on the bottom of a gas oven (it interferes with combustion)
- never operate an unvented gas-burning appliance in a closed room, especially a room in which you sleep
- keep CO-producing devices away from open windows and doors or vents of the home. NWJ

For additional information see the US Product Safety Commission's web site: www.cpsc.gov.

Point of View, continued from page 1

laboratories. I know of no other weapons systems, or for that matter, any other government procurements at all, that are validated in this manner.

The University of California's contributions at Los Alamos over the past 63 years range from the development and stewardship of a safe and secure nuclear deterrent that has been successful in preventing major war to the successful development of a spectrum of other national defense-related technologies that serve or stand ready to serve. UC has also established a scientific capability that is second to none in protecting the nation from technological surprise and contributing to other national challenges and priorities. And finally, UC has created a paradigm for academic service in the public interest that serves the nation well and is unequaled anywhere.

These virtues will continue to be nurtured and strengthened at Los Alamos as the UC partnership enters a new era and takes the Laboratory to the next level of performance. I have no doubt that the nation's science-based RRW and related nuclear weapons infrastructure will continue the extraordinary success that began with Robert Oppenheimer, UC, and Little Boy. NWJ

Robert W. Kuckuck was appointed director of Los Alamos National Laboratory effective May 16, 2005, and served as director until May 31, 2006. He was the eighth director of the Laboratory.

Dr. Kuckuck worked at Lawrence Livermore National Laboratory for more than 35 years, holding a number of management positions that included deputy director of the laboratory from 1994 to 2001.

He received his doctorate in applied science from the University of California, Davis, and his master's degree in physics from Ohio State University. He did his undergraduate work in physics at West Liberty State College.

In 2003, Dr. Kuckuck received the Department of Energy Secretary's Gold Award, DOE's highest honor. The award citation by Energy Secretary Spencer Abraham recognized him for "superior leadership" and for "vision, dedication and commitment to excellence…that have directly resulted in the advancement of initiatives that are strengthening the nuclear security of the United States of America."

A BACKWARD GLANCE

Operation Castle

The US detonated its first full-scale thermonuclear test shot, code-named Mike, on October 31, 1952, as part of Operation Ivy. Mike produced a yield of 10.4 MT, the equivalent of 800 Little Boy bombs (the type used to destroy Hiroshima at the end of World War II). But Mike was a large, unwieldy test device that could not be delivered in combat. Over the next year and one-half, the US developed deliverable bombs based on principles demonstrated in the Mike test. This first generation of thermonuclear weapons was tested in the spring of 1954. The test series, Operation Castle, included six shots, five of which were in the multimegaton range.

The 11-MT Romeo blast.

Shortly before Mike was tested, the Joint Chiefs of Staff issued a directive calling for the development of a deliverable hydrogen bomb that would be ready for deployment in 1954. The original schedule called for testing several potential designs in late 1953. But just after the test series was announced, it was delayed. Los Alamos scientists, led by J-Division Leader Alvin C. Graves, argued that thermonuclear tests were too large to be conducted at the Marshall Islands' Enewetak Atoll, the projected testing location. Therefore, the Bikini Atoll, east of Enewetak although still in the Marshall Islands, was adopted as the test site despite its lack of support structures. Completion of these facilities pushed Castle's start date to the early spring of 1954.

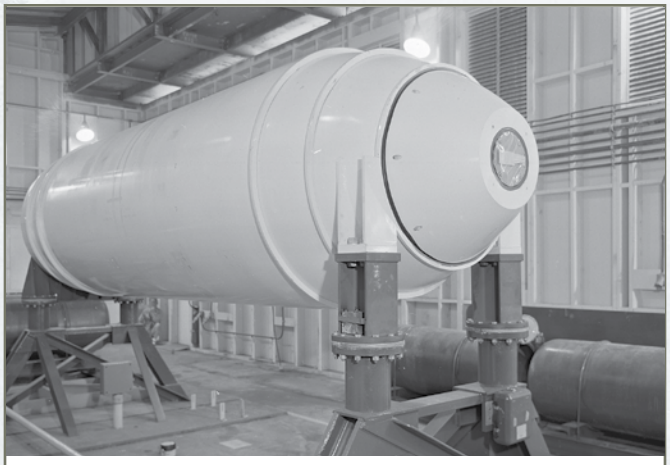

A device that was tested in 1954 as part of Operation Castle.

The first Castle shot, code-named Bravo, was fired in February 1954. Bravo was expected to have a yield of 6 MT; as the massive fireball expanded, it became clear that Bravo was a great success. However, radiation levels in the area began to rise rapidly, and feelings of achievement soon turned to apprehension. Bravo was more than twice as powerful as expected—a staggering 15 MT, the largest blast in the history of American testing. The shot generated unprecedented amounts of fallout, necessitating the evacuation of hundreds of Marshallese Islanders. The crew of a small Japanese boat, ironically named the Lucky Dragon, also fell victim to the fallout. These events escalated international concerns about atmospheric testing, which eventually resulted in the testing moratorium of 1958.

Castle continued as scheduled, despite the problems encountered with Bravo. The Bravo shot confirmed the practicality of a dry-fuel weapon, which was far lighter and much easier to deliver than a wet-fuel model. This breakthrough in design prompted Harold Agnew, the director of two subsequent tests, to send the coded message, "Why buy a cow when powdered milk is so cheap." In fact, the dry-fuel devices were so successful that they rendered the wet-fuel devices obsolete and the only wet-fuel design was scratched.

Testing resumed in March with Romeo, which obtained a yield of 11 MT. A Lawrence Livermore Laboratory design (a 110-kt fizzle) was tested next. In late April and early May three final shots, all Los Alamos designs, were carried out: Union, Yankee, and Nectar obtained 6.9-, 13.5-, and 1.7-MT yields, respectively, bringing the nation's first major thermonuclear test series to a close. NWJ

Point of contact:
Alan Carr, 664-0870, abcarr@lanl.gov